L28.

AN EXPERIMENTAL INVESTIGATION INTO THE PERFORMANCE OF A SMALL HORIZONTAL CYCLONE COMBUSTION CHAMBER AS A COLD AIR AND HOT AIR MODEL AND AS A PROTOTYPE FURNACE

A THESIS

By

KALIPADA PALIT

Submitted to the Department of Mechanical Engineering of East Pakistan University of Engineering and Technology in partial fulfilment of the requirements for the degree of Master of Science in Mechanical Engineering.

September, 1968.

This is to certify that this work was done by me and it has not been submitted elsewhere for the award of any degree or diploma or for publication.

Valentino .... Kalipada Pahit ....

(Signature of the supervisor) (Signature of the candidate)

ACKNOWLEDGEMENTS

The author expresses his profound gratitude to Dr.Valentine Gerald DeSa for his constant supervision of this research. His continued advice, inspiring guidance, help and encouragement have been a valuable aid in completing the work.

The author takes this opportunity to extend his sincere appreciation to Dr. M.H.Khan for his valuable suggestions and directions in the preparation of the work.

The author gratefully acknowledges the kind assistance of Dr. Shamsul Alam in several aspects of this research.

The author expresses his sincere thanks to all those who assisted him in various spheres of the research. Special thanks are also due to Mr.Jaffarbhai Basrai and Mr.Md.Anisuzzaman for their kind help in carrying out the experimental programme, of the research.

ABSTRACT

This research is an experimental investigation into the performance of a small horizontal cyclone combustion chamber used as a cold air and hot air model and as a prototype furnace. The cyclone combustion chamber was built up by the author; the set-up consisted of a 100 cfm radial air blower, a 21 kw electric preheater for secondary air, a gravity controlled fuel feeding hopper and the 12 in. diameter combustion chamber with nozzles for admitting primary air and fuel particles and the secondary air. Velocity probes and static pressure probes were installed at different sections of the combustion chamber for study of the flow pattern, velocity distribution and pressure losses when used as either a cold air or hot air model. Thermocouples were also mounted for determining the temperature distribution in the hot air model and prototype furnace.

The primary air and secondary air entered tangentially into the cyclone combustion chamber. It was found from earlier experience with this unit that, for transport of fuel particles of a particular fineness in suspension in the primary air, there was a certain optimum value of the velocity of the primary air. Also it was observed from earlier studies that there was a range of secondary air velocities within which ignition and combustion was practicable. Consequently, in this series of experiments the primary air flow was kept constant and secondary air flow varied within these limits. In the hot air model and in the prototype furnace tests, the secondary air was preheated to a temperature of 500 °F. The prototype furnace was fired with peat coal of finenesses ranging from 8-mesh to 100-mesh.

From the experimental investigation, it has been found that the fluid flow in the cyclone combustion chamber was spiral, with the axial flow velocity pattern somewhat similar for the cold air model and hot air model; near the surface of the chamber wall the flow was in a layer form whilst at the central zone there was negligible flow, except at the throat. The intensity of turbulence varied in the air models,depending on the secondary air velocities; in the prototype furnace more intense turbulence developed because of high heat release and radiative heat transfer. The hot air model and the prototype furnace did not yield the expected similarity of temperature distribution inside the cyclone combustion chamber. Hence air models, inspite of the geometrical similarity and similarly Reynolds numbers do not predict results as obtained in the prototype furnace, because of the increased turbulence,and the radiative and convective heat transfer associated with high rates of heat release with combustion of fuel. The effect of these parameters must be included in the design of the air models,if these are to predict satisfactorily the performances of the prototype furnaces.

In tests on the combustion characteristics of the prototype cyclone furnace, it has been found that for a given primary air velocity flow, the size of the fuel particles and the secondary air velocity influence largely the ignition and extinction phenomena of cyclone combustion. The ignition temperature decreased with a decrease in the size of fineness of the fuel particles; so also did the flame length as the particles burned near the nozzles. The burning time for the coarser fuel was larger, and combustion of these particles took place nearer the throat. Increase in secondary air velocity accelerated the rate of combustion upto a certain limit beyond which the chamber temperature begins to fall and ultimately extinction occurs. The extinction temperatures are higher than the ignition temperatures,and whilst this phenomena has been theoretically predicted by Vulis(41), the author has not found any references of such experimental results. Combustion of finer fuel particles took place nearer the nozzle and that of coarser particles near the throat. It is anticipated that kinetic combustion occurred in the earlier part of the combustion chamber and diffusion combustion in the latter part of it.

The experimental cyclone chamber is an useful tool for determining the limits of applicability of air models for furnace design as well as for combustion studies.

TABLE OF CONTENTS

CHAPTER 1

INTRODUCTION

1.1 This report presents the results of an experimental investigation into the performanee of a small horizontal cyclone combustion chamber used as a cold air and hot air model and also as a prototype furnace.

1.2 The cyclone furnace was developed as a part of research programme on solid fuel firing for gas turbines. In recent years, gas turbine application has assumed less importance and the main emphasis of work has been on studying the performance of the cyclone combustor with a variety of coal, widely used for steam power stations.

1.3 The cyclone furnace is an outstanding equipment which helped the development of the combustion chamber. The firing of pulverised fuel has now become more applicable than stoker firing. Since caking properties do not effect the combustion performances in the pulverised fuel firing; pulverised fuel flames can burn low grades of coal and also easily respond to the fluctuations of load. But the difficulties arise while removing the fine grained fly ash. These difficulties led to the development of the furnaces in which ash was produced in a granulated and a salable form. Now, the present trend in the development of the combustion technique is towards liberation of maximum energy in the smallest possible space. In an endeavour to remove the difficulties of ash handling and also to liberate maximum energy contained in the fuel in the smallest space, a system of burning pulverised coal in vortex suspension has recently been developed. The system comprises a cylindrical combustion chamber having an inlet for fuel and air at one end and a gas discharge throat at the other end. Primary air admitted tangentially to the cylinder carries the fuel particles. Secondary air is also admitted tangentially at a comparatively higher velocity to create a strong vortex. Extremely high heat liberation causes high temperature inside the combustion chamber. The fuel is quickly consumed and ash forms a molten film flowing over the inner wall of the cylinder. The molten ash flows to an appropriate disposal system.

1.4 Extensive investigations into the performances of the cyclone furnaces are still in progress. Efficient combustion within the cyclone chamber largely depends on the formation of swirl. The secondary air velocity, the length and diameter of the cylindrical combustion chamber determine the length of the swirl. Adjustment of all these parameters results in efficient combustion. Since the process of burning pulverised fuel generates heat in a moving gaseous medium, aerodynamics and thermodynamics become inseparably linked. Comprehensive investigations into the aerodynamics of a horizontal cyclone furnace were carried out by Cautius (7) and Siedl (34). According to Cautius, the flow in the cyclone can be split up into tangential, radial and axial velocities of which the behaviour of the axial component is the least known. Cautius attempted by model tests to investigate the axial flow in the horizontal cyclone. It was observed that with the tangential admission of the primary and the secondary air through the nozzles, swirl was developed within the cylindrical chamber. The swirl moved forward in the form of an increasing pitch helix. The fuel particles were introduced suspended in the primary air stream. On entering into the combustion chamber, the larger sizes were separated by the centrifugal force and deposited on the wall of the combustion chamber. Smaller sizes moved in vortex suspension. Lobscheid (21) attempted to measure the pressure losses in the combustion chamber. An accurate measurement was not possible because of the complicated flow inside the combustion space. It was found that the pressure loss in the combustion chamber consisted of the pressure loss in the nozzle, the pressure loss in the vortex and the pressure loss during combustion.

1.5 Hoy, Roberts and Wilkins (14) carried out investigations with a horizontal cyclone furnace. They studied the effect of fuel size, fuel type, secondary air velocity, secondary air temperature and air fuel ratio on the process of cyclone combustion. It was observed that the velocity of secondary air was of paramount importance as it effected the distribution and movement of the particles within the cyclone, their subsequent rate of burning and also the movement of the slag. In addition, it determined the pressure losses. It was found that the effect of fuel size had also an appreciable influence on the process of combustion. Increasing the quantity of fines increased the amount of fuel burning in suspension and hence, the tendency for more particles to escape from the cyclone. This was apparently counter-balanced by more rapid combustion of these particles. A more fluid surface to the slag layer was also probable with the finer grinding since this resulted in more rapid ignition and caused the ash to be in a finer state of division when it reached the wall.

1.6 Combustible mixure forms a heterogeneous system within the cyclone furnace. Kinetic and diffusion combustions occur simultaneously within the combustion chamber. In both kinetic and diffusion combustion, ignition and extinction of the combustible mixture occur under certain defined conditions. Kinetic combustion prevails in the regions of low temperature,higher air velocities and smaller particle sizes. Diffusion combustion prevails in the regions of higher temperature, lower air velocity and larger particle sizes. There are certain limiting values of the air velocity and the particle size at which combustion will be stable throughout the length of the combustion chamber.

1.7 Experimental investigations on a full size cyclone furnace being enormously expensive of time, money and material, technique of modeling has been adopted most recently to predict the results of the prototype furnaces. Moreover, cyclone combustion is so complex that some accurate measurements of all the variables were too difficult to be made. Hot and cold air models are conveniently used for combustion model study. Cold model is capable of giving both qualitative and quantitative information about flow conditions in the prototype furnaces. The hot model and the prototype furnaces will have similar temperature profiles. In the present investigation, a small horizontal cyclone furnace has been used as a cold model and also as a hot model.

1.8 In the subsequent chapters of this report, details of theory of cyclone firing, thermal theory of cyclone combustion, modeling of cyclone furnaces,experimental method, results and discussion have been presented.

CHAPTER II

THEORY OF CYCLONE FIRING

2.1 This chapter is devoted principally to the study of flow of gas and fuel particles inside the cylindrical combustion chamber of a cyclone furnace. The flow of gas covers mode of admittance and distribution of air and the development of cyclone flow. The flow of fuel particles concerns how the fuel particles enter into the combustion space after being mixed with hot air stream, how they diminish in size when these burn in the combustion chamber and, finally, how they are separated from the slag; the limiting size of the fuel particles is discussed in this context. Mixture formation is also explained. Finally, the parameters influencing the pressure losses in the cyclone chamber are presented.

2.2 A cyclone furnace (Fig.2-1) basically consists of a cylindrical combustion chamber, fitted with nozzles for admitting fuel and air inside the combustion space.Some of the nozzles are meant for admitting air carrying fuel particles in suspension and others for admitting only air.

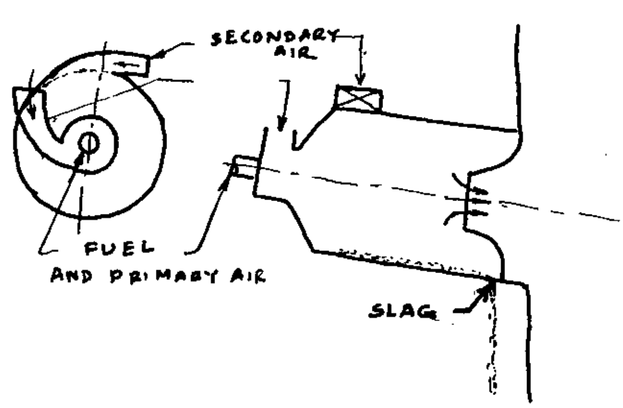

Fig. 2-1. Diagram of a cyclone furnace. (32)

Usually the air carrying the fuel is termed as 'Primary air' and the air which enters the furnace on being preheated is termed as 'secondary air'. In some cyclone furnaces, 'tertiary air' is also supplied to provide a velocity component in the direction of the secondary furnace and to ensure burning of any fuel particle suspended near the centre of the vortex flow pattern. The cyclone combustion chamber is divided into two by a throat. The major part before the throat, where combustion occurs mainly, is known as Primary combustion chamber and the rear part after the throat is known as Secondary combustion chamber where the products of combustion may be diluted if necessary by admitting more air. According to positioning, a cyclone furnace may be vertical, horizontal and inclined, the axis of the cylindrical combustion chamber of the cyclone furnace being the criteria for distinguishing between different configurations. Our major attention is focussed on the horizontal cyclone furnace.

FLOW OF GAS AND FUEL PARTICLES

2.3 In the cyclone system of combustion, the primary air is usually fired tangentially into the cylindrical combustion chamber. Secondary air, about 75 to 80 % of total air is also admitted tangentially at higher velocity and creates a strong vortex highly turbulent and provides a thorough mixing of fuel, air and combustion products in the horizontal cyclone. With this tangential admission, a mixture swirl is formed which moves along the cylindrical wall of the combustion chamber in the form of an increasing pitch helix. The crushed coal fuel is conveyed to the chamber by the primary air and on entering tangentially, the majority of the fuel particles are centrifuged to the walls and burn thereupon. By using airfuel ratios near to the stoichiometric and heating the secondary air for combustion, a high combustion temperature results with extremely high heat liberation. The fuel is then quickly consumed and the ash melts. The centrifugal force resulting from admitting the primary and secondary air throws the molten ash to the periphery of the cylindrical wall.The liberated ash forms a molten film flowing over the inner wall of the cylinder. A thin layer of ash solidifies on the comparatively cooled walls of the chamber and attains an equlibrium thickness which is determined by the temperature of the combustion gases and the temperature at which ash flows freely. Fuel particles are trapped and embedded in the film of sticky slag and are subjected to an intense scrubbing action as the air sweeps over the coal. Fuel particles above a certain size burn on the slag layer and others below this size keep burning in suspension. The fuel particles while flowing thus diminish in size. Liquid ash (slag) flows down the surface of the solidified layer to an outlet at the bottom of the combustion chamber. The slag layer restrains the movement of those coal particles reaching the wall surface and the resulting relative motion between air and air and fuel particles results in high combustion intensity. About 80 to 85 % of the ash leaves the combustion chamber as slag and hence the combustion gases contain only a small portion of the ash. The ash free products of combustion flow through the throat into the secondary combustion chamber.

Development of Cyclone Flow

2.4 The cyclone flow theory is still based on isothermal conditions and, therefore, as a first approach the potential theory can be applied. The flow in the cyclone can be split up into tangential, radial and axial velocities of which the behaviour of the axial component is the least known. Cautius(8) attempted in model tests to investigate the axial flow in the horizontal cyclone with the results shown in Fig. 2-2. On injecting the fuel near the cone of the cyclone the result was a loop like axial flow and this was confirmed by the Russian tests carried out in 1958 by Knorre and Nadzharov(20).

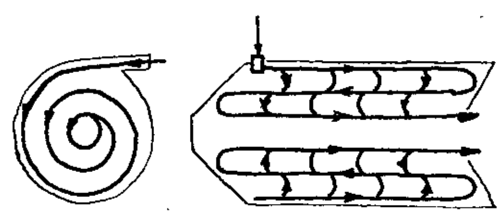

Fig. 2-2. Axial flow pattern in a horizontal cyclone furnace. (31)

2.5 The flow in a cyclone is basically composed of a sink and a vortex. If Q be the streaming gas quantity through a circular cross section of radius r_0 such that

$$Q = 2\pi L r v_r = 2\pi L r_o v_{r_o} \qquad (2\text{-}1)$$

where L = length of the cylindrical combustion chamber

r = any radius of the cylinder

the radial velocity is $$v_r = \frac{v_{r_o} r_o}{r} \qquad (2\text{-}2)$$

and similarly the peripheral velocity due to the whirl is

$$u_r = \frac{u_{r_0} r_0}{r} \qquad (2\text{-}3)$$

The resultant velocity vector makes an angle of α with the circumferential velocity such that

$$\tan\alpha = \frac{v_r}{u_r} = \frac{v_{r_0}}{u_{r_0}} = \text{Constant} \qquad (2\text{-}4)$$

The angle is also constant. On the otherhand,

$$\tan\alpha = \frac{dr}{r\,d\varphi} \qquad (2\text{-}5)$$

wherefrom,

$$r = r_0\, e^{c\varphi} \qquad (2\text{-}6)$$

The Eqn.(2-6) exhibits a logarithmic spiral. Fig. 2-3 shows the possible flow in a cyclone.

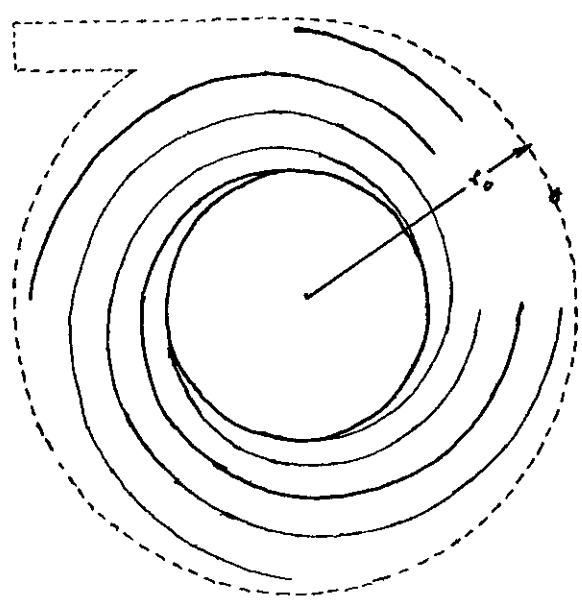

Fig. 2-3. Flowfield in a cyclone. (7)

Limiting Size of Fuel Particles

2.6 Here interest lies chiefly with the motion of those particles that do not lie at the cyclone periphery. Some portion of these particles flow away with the volatile ingredients into the centre of the vortex, but the greater portion remains on the circular orbit of the cyclone. The particle for which the centrifugal force and the drag force of the central vortex are in eqgilibrium and which does not make any radial movement is called the particle of limiting size, being at the limit of separation possibilities. The minimum size of particles, which can not be separated by the centrifugal force but will be transported by the flue gases flowing to the cyclone outlet, can be calculated as follows

$$\psi \left(\frac{\pi d^2}{4}\right)\left(\frac{v_r^2}{2g}\right)(\gamma_{fg}) = \frac{\pi d^3}{6}\left(\frac{u_r^2}{r}\right)\left(\frac{\gamma_f}{g}\right) \qquad (2\text{-}7)$$

where $\psi = \dfrac{24\nu}{d\, v_r}$

ν = kinematic viscosity

γ_{fg} = specific weight of the flue gas at the standard temperature

γ_f = specific weight of coal

μ = dynamic viscosity of coal

$$\mu_t = \mu_0 \left[\frac{\left(1+\frac{c}{273}\right)}{\left(1+\frac{c}{273+t}\right)} \sqrt{\frac{273+t}{273}}\right] \qquad (2\text{-}8)$$

C = Sutherland constant

μ_0 = Dynamic viscosity at normal temperature

μ_T = dynamic viscosity at any temperature

$$v_r = \frac{Q_{fg}}{2\pi r_f l} \qquad (2\text{-}9)$$

where Q_{fg} = flue gas rate

l = active whirl length

From Eqn.(2-7) and (2-9),

$$d = \frac{3r}{u_{r_0} r_0} \sqrt{\frac{\nu Q_{fg} \gamma_{fg}}{\pi \gamma_f l}} \qquad (2\text{-}10)$$

2.7 The limit particle circulates therefore on a circle of the size of the outlet throat. There is simple formula for the drag force, F_d if the same is expressed in terms of γ

dependence on the velocity at which the particle will float. According to Fig. 2-4, the drag force, F_d and the centrifugal force, F_c are equalised. From that the particle-balance

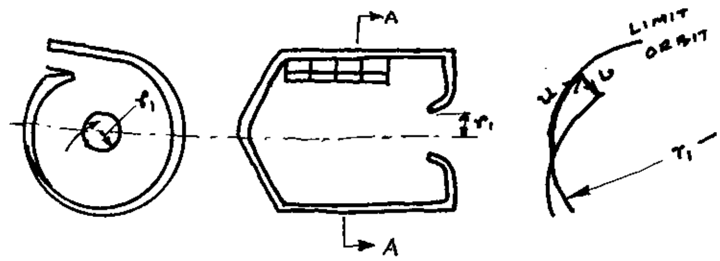

Fig, 2-4. Limiting particle size for separation in cyclone. (34)

velocity that is the velocity at which the particle floats is calculated and the corresponding size of the dust particle or slag droplet can be determined from the usual diagram depending on the flue gas temperature and specific gravity of the particle. In the limit orbit condition,

$$F_d = F_c$$
$$\frac{m g v_r}{v_b} = \frac{m u_r^2}{r_1}$$
$$v_b = \frac{g r_1 v_r}{u_r^2} \qquad (2\text{-}11)$$

where m = mass of the particle

r_1 = radius at gas outlet

v_b = velocity at which the particle floats

v_r = gas radial velocity

u_r = gas tangential velocity

The theoretical slag separation efficiency of a furnace cyclone can be expressed as a certain rate of the total quantity of particles being bigger than limit particle size. This slag separation efficiency is greater the more coarsely the fuel has been pulverised, 2.8 A coarse grinding rather than the limiting size of the fuel particles is, therefore, a pre-requisite for the separation and combustion upon a slag bed. The observations show that capturing the particles of coal is made easier near the periphery of the separator with significant angular momentum and tangential velocity.

MIXTURE FORMATION

2.9 With the mixing of two gases, e.g. air with the burning gases, the material exchange through the volume element resulting from the diffusion across the flow and from the flow itself can be found out.

2.10 If the concentration field in the combustion chamber $c = f(x, y, z)$ and the gas velocity field $w = f(x, y, z)$ are known, the equation for the flow can be worked as

$$q = D \frac{\partial c}{\partial x} \qquad (2-12)$$

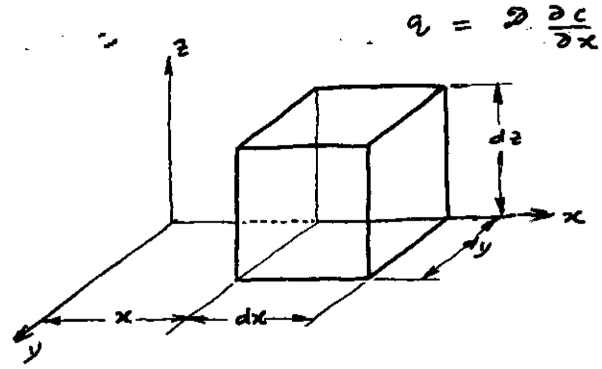

Fig. 2-5. Material exchange through the volume element. (7)

By comparison with the Fig. 2-5, the velocity is

$$w_x + \frac{\partial w_x}{\partial x} dx$$

the concentration is

$$c + \frac{\partial c}{\partial x} dx$$

and the concentration gradient is

$$\frac{\partial c}{\partial x} = \frac{\partial^2 c}{\partial x^2} dx$$

then the concentration exchange through the volume element is

$$\frac{\partial c}{\partial \tau} = \mathcal{D} \Delta c \qquad (2\text{-}13)$$

where $\mathcal{D}$ = diffusivity factor

Δ = Laplacian operator

The concentration gradient can also be written as

$$\frac{\partial c}{\partial \tau} = c \operatorname{div} \omega + \omega . \operatorname{grad} c \qquad (2\text{-}14)$$

With the help of dimensionless parameters,

$$\xi = \frac{x}{D} ; \ \eta = \frac{y}{D} ; \ \zeta = \frac{z}{D}$$

where D = the combustion chamber diameter

V_R = the relative velocity

the mixing loss or the leakage error is

$$\varphi = \left(\frac{c_\ell}{c_m} - 1\right) \qquad (2\text{-}15)$$

where c_ℓ = the local concentration with reference to the measuring volume

c_m = the concentration exhibited in the middle of the cross section

Introducing further

τ_0 = the reference time

τ = the dimensionless time

ω = the dimensionless velocity vector with the components ω_x, ω_y and ω_z

L = the length of the combustion chamber

the equation can be worked out as

$$\frac{\partial \varphi}{\partial \tau} = \frac{A \tau_0}{D^2} \Delta \varphi + \frac{L}{D} (\varphi + 1) \operatorname{div} \omega + \frac{L}{D} \omega . \operatorname{grad} \varphi \qquad (2\text{-}16)$$

Here the characteristic factor, $\frac{D^2}{A \tau_0}$ which is equal to F_0 occurs in the inverse form in the above equation in coherence with that of the heat conduction process as a

Fourier characteristic factor.

2.11 With a constant volume combustion chamber,

$$\operatorname{div} \omega = 0$$

If further the material exchange is preferably normal to the flow, $\omega \cdot \operatorname{grad} \varphi = 0$

the Eqn.(2-16) becomes

$$\frac{\partial \varphi}{\partial \tau} = \frac{1}{F_o} \cdot \Delta \varphi \qquad (2\text{-}17)$$

and this is identical with the Fourier equation of heat conduction. F_o has an analogous significance for the mixture formation as N_{Re} has for the flow processes. From this equation, it can be recognised that the short burning time and high combustion chamber loading necessiate small diameter of the combustion chamber.

PRESSURE LOSSES IN CYCLONE CHAMBER

2.12 A correct computation of the pressure ratio is not possible because of the complicated flow inside the combustion chamber. The most difficult is to determine the frictional losses. The formula given below is built upon an ideal condition and gives an overall idea of the pressure losses and its distribution in the cyclone. Lobscheid (21) attempted to arrive at a correct computation determination of this ratio of the cyclone. He introduced a co-efficient which he took from an already existing system. The pressure loss is composed of the pressure loss in the nozzle, pressure loss at the vortex, pressure loss for combustion.

Pressure Loss in the Nozzle

2.13 The nozzle pressure loss is

$$\Delta P_N = \frac{\rho}{2}\left(\frac{V_g}{C_d a}\right)^2 \qquad (2\text{-}18)$$

where V_g = actual gas volume

C_d = co-efficient of discharge

a = Narrowest nozzle cross section

ρ = density of the flue gas at the existing temperature

Pressure Loss in the Vortex

2.14 The pressure loss in the whirl is calculated from the basic equation of the flow through a volume element. The basic equation is

$$\frac{du}{dr} + \frac{u}{r} = 0\ ; \quad \frac{u}{c} = \frac{1}{r}\ ; \quad u = \sqrt{\frac{2\Delta P_V}{\rho}} \qquad (2\text{-}19)$$

$$\Delta P_V = \frac{\rho}{2}\left[\left(\frac{D}{D'}\right)^2 - 1\right] u_o^2$$

where D = the diameter of the cyclone

D' = the diameter of the nozzle tip

u_o = tangential velocity at the cyclone wall

The calculated pressure drop results from the equation ur = constant. From the established results of the model studies, it appears as admissible to apply also the equation for the vortex as ur^2 = constant.

2.15 The real existing pressure loss does not follow either of these two equations. One could, therefore, think of setting an equation such as ur^p = constant, where p lies between 0 to 1. It is obvious only that the exponent of the above two equations can be successfully taken as ½ from which results as $$\Delta P_v = \frac{u_o^2 \rho}{2}\left(\frac{D}{D'} - 1\right) \qquad (2\text{-}20)$$

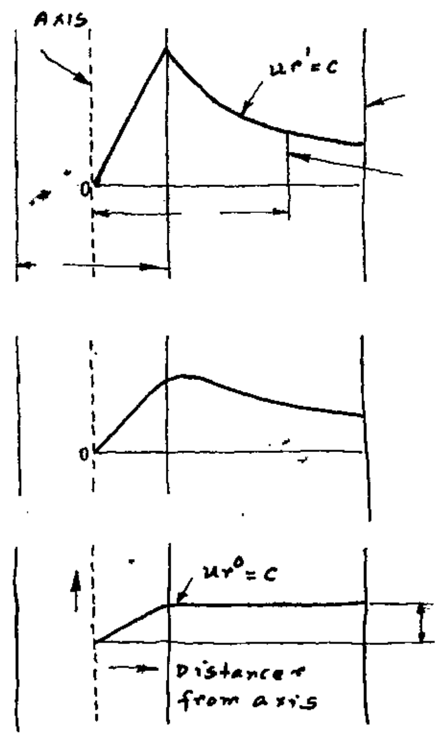

Fig. 2-6. Rotating velocities in section of cyclone. (34)

2.16 Furthermore, Fig. 2.6 shows the flow of vortex in the cyclone furnace under various possible conditions. The correct potential vortex with the equation ur = constant does not occur. Measurements have shown that there occurs a flow ur^x = constant where x = 1/2 and with simplified acceptance also ur = constant. In this formula, u is the circumferential velocity at radius r and r is the distance from the cyclone axis. The deviation from the potential or ideal vortex is to be explained by the content of coarse dust in the gases, by means of which their velocity is altered. Fig. 2-6 shows the comparison of the three forms of flow. The rotating velocity u is shown as ordinate and the distance as abscissa.

2.17 The maintenance of the flow forces which affect the coal particles and the slag droplet respectively is done from the available pressure head at the cyclone inlet. Measurements resulted in the following subdivided pressure losses :

VALUES FOR SEIDL'S HORIZONTAL CYCLONE FURNACE

	mm.W.G.
For producing the circumferential velocity of 100 m/sec(maintenance of the centrifugal power)	450
For maintaining the gas movement radially from the outer wall zone to the cyclone centre (maintenance of the central vortex)	120
For conveying the gases through the discharge throat	230
Total	800

The small amount of pressure of only 120 mm of w.g. for the flow from the outer wall zone to the cyclone centre shows that there is no essential increase of velocity to the centre. It is found that the pressure loss is the highest for a pure potential vortex.

Pressure Loss during Combustion

2.18 If the surface friction is omitted in the case of exit of the combustion gases, the pressure loss during combustion, ΔP_c stands from the theory of impulse as,

$$\Delta P_c = \frac{1}{2}\frac{u_a^2}{\rho_o}\left(\frac{\rho V_g + \frac{W_f}{g}}{\varphi V_a}\right) \qquad (2\text{-}21)$$

where ρ_a = density of secondary air

V_a = secondary air volume

v = exit velocity of the air at the tip of the nozzle

C_v = co-efficient of the velocity for nozzle tip

W_f = coal rate

The summation of the pressure losses gives the combined pressure loss as follows

$$\Delta P = \Delta P_N + \Delta P_v + \Delta P_c \qquad (2\text{-}22)$$

and, therefore, the tangential velocity results as

$$u_o = \frac{\Delta P - \frac{\rho}{2}\left(\frac{V_g \, D'^{4}}{\cdot 785 \, C_d}\right)^2}{\frac{\rho}{2}\left[\left(\frac{D}{D'}\right)^2 - 1\right] + \frac{1}{2\rho_o}\left(\frac{\rho V_g + \frac{W_f}{g}}{\varphi \, L}\right)^2} \qquad (2\text{-}23)$$

2.19 In the present chapter, we have analysed the flow of gas and fuel particles in the cylindrical cyclone chamber. The tangential admission of primary and secondary air through the nozzles into the combustion chamber develops a cyclone. This cyclone is basically a logarithmic spiral and it follows the equation, $r = r_o e^{c\varphi}$. Because of the horizontal configuration of the furnace, it also traverses along the wall of the cylinder in the form of an increasing helix. The design of the cyclone furnace should be such that sufficiently long swirl would be developed inside the combustion space to ensure combustion of the fuel particles. Usually the fuel particles above a certain size are trapped in the sticky slag layer at the wall of the combustion chamber and burn thereon. Others below this size burn in vortex suspension. The fuel particles diminish in size as these keep on [illegible] flowing. The critical size of the fuel particle is $d = \frac{3r}{u_{r_o} r_o}\sqrt{\frac{\nu \, a_{fg} \, r_{fg}}{n \, r_f \, l}}$

In the process of mixing of air with the fuel particles, pressure losses occur. The total pressure loss in the cyclone chamber is the summation of the pressure losses in the nozzles, vortex and during the combustion process. The pressure loss in the nozzles is considerably greater than those in the others. In the following chapter, we shall discuss the thermal aspects of cyclone combustion.

CHAPTER III

THERMAL THEORY OF CYCLONE COMBUSTION

3.1 Earlier, we have dealt with the hydrodynamic aspects of cyclone combustion, especially the flow of gas and fuel particles. There remains an examination of the thermal aspects of cyclone combustion before dwelling on modelling on combustion chambers. In a cyclone furnace, combustion is an exceedingly complex heterogeneous physico-chemico process, associated with a large number of variables. This necessiates a simplified analysis using nondimensional parameters which are introduced in this chapter. Such an analysis makes feasible the presentation on a kinetic basis, of the concepts of possible stationary levels of the process and the phenomena of ignition and extinction, whilst the possible steady states and the possibility of existance of critical ignition and extinction regions are explained assuming diffusion combustion. The thermal process in the cyclone combustion chamber and the parameter influencing it are finally presented in their totality.

HETEROGENEOUS COMBUSTION

3.2 In a cyclone furnace, the mixture components constitute a two-phase system and, hence, the combustion of air and fuel particles in the combustion chamber is a heterogeneous process, neither exclusively kinetic nor diffusional and, in the general case, both kinetic and diffusional combustions are prevalent. Combustion is kinetic when the physical mixing of fuel and sufficient amount of combustion air takes place earlier and outside the combustion space; the rate of kinetic combustion depends only upon the chemical reaction velocity. Diffusion combustion results when fuel and air are introduced separately into the combustion space and fuel burns as it mixes with the air; rate of burning depends upon the rate at which oxygen reaches the fuel and, thus, in turn depends on the flow pattern and degree of turbulence in the combustion space. Kinetic combustion prevails in the regions of low temperature, high values of air velocities and large particle sizes.

3.3 Kinetic and hydrodynamic factors influence the cyclone combustion process. These are temperature of combustion, the heat of reaction, the heat capacity of the combustion products, extent of completeness of combustion, concentration of the combustible mixture, stay time of the mixture in the combustion chamber, diffusion time and characteristic reaction time of the mixture. In nondimensional parameters, these factors can be expressed as follows.

3.4 Nondimensional concentration of the combustible mixture is defined as

$$\bar{c} = \frac{c}{c_o} \qquad (3\text{-}1)$$

where c = the concentration of the combustible mixture in the combustion region

c_o = the initial value of the combustible mixture concentration

The co-efficient of completeness of combustion is related thereto

$$\varphi = 1 - \bar{c} \qquad (3\text{-}2)$$

The value of φ is numerically equal to fraction of heat liberated during the reaction process. The quantity of heat liberated during the combustion process is expressed by Arrhenius equation

$$Q_1 = A\, e^{-E/RT} \qquad (3\text{-}3)$$

where Q_1 = the quantity of heat liberated in the combustion chamber

A = numerical constant

E = activation energy

R = universal gas constant

T = temperature of combustion

RT/E is defined as nondimensional temperature, θ .Use of this variable permits a simplified reaction analysis for mixtures with different values of activation energy. However, another characteristic is needed for comparison of reactions with mixtures of varying average specific heat and, also, for estimating the influence of an excess of one of the components of the combustible mixtures. Such a nondimensional variable is the reduced heat production of the mixture and is expressed as

$$\nu = \frac{R q C_0}{E C_p} \qquad (3\text{-}4)$$

where q = the heat of reaction

c_p = constant heat capacity

Hydrodynamic factors are associated with the mixture stay time, gas diffusion time and the reaction time. It is, therefore, convenient to take the ratios of the mixture stay time, τ_s the time τ_D required for gas diffusion to the reacting surface, and the time, τ_K for the chemical reaction to progress on the latter. The nondimensional time τ_{SK}, τ_{DK} and τ_{SD} are expressed as

$$\tau_{SK} = \frac{\tau_s}{\tau_K}\ ; \quad \tau_{DK} = \frac{\tau_D}{\tau_K}\ ; \quad \tau_{SD} = \frac{\tau_s}{\tau_D} \qquad (3\text{-}5)$$

3.5 With combustible mixtures in a cyclone chamber, the stability of flame and combustion depends on two contending processes-the first a process of heat liberation, associated with heat of reaction of the mixture and the second a process of heat elimination whereby heat is carried away by the products of combustion and mixture. In the course of analysis, the ω-θ co-ordinate system affords a convenient graphical representation of the process of cyclone combustion. The heat liberation curve, $\omega_J = \varphi(\theta)$ for the combustible mixture in the $\varphi - \theta$ diagram is generally an S-shaped curve (Fig.3-1). The heat elimination curve, $\varphi_D = \varphi(\theta)$ on the co-ordinates is on the other hand an inclined straight line (Fig.3-1). The shape of the heat liberation curve and the slope

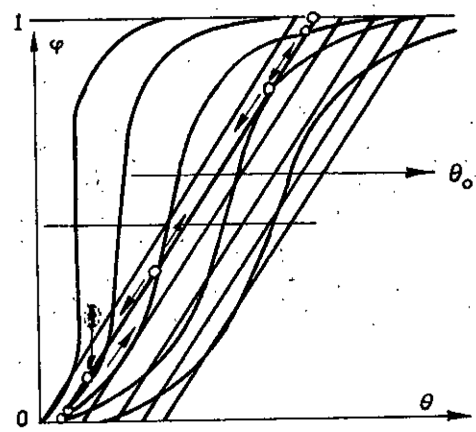

Fig. 3-1. Curves of completeness of combustion, as a function of temperature, .(41)

of the heat elimination line vary for different conditions of cyclone combustion. The points of intersection of the heat liberation and the heat elimination curves determine the stationary regions or steady levels of cyclone combustion, since amount of heat liberated by combustible mixture at these points of intersections is exactly equal to the amount of heat eliminated with the combustion products. The point of tangency of these curves in the range of lower values of φ and θ is called the point of ignition and at the higher values of φ and θ is called the point of extinction or collapse of combustion flame. In the subsequent sections, the subscript 'o' stands for the initial conditions, 'I' for ignition, 'E' for extinction, 'cr' for the critical conditions and 'st.' for the stationary values of the parameters.

<u>Kinetic Combustion</u>

3.6 The rate of kinetic combustion depends exponentially on the temperature and heat of reaction of coal. All the heat liberated because of reaction within the chamber is transformed completely into the heat capacity of the combustion products. In otherwords, combustion is steady and adiabatic.

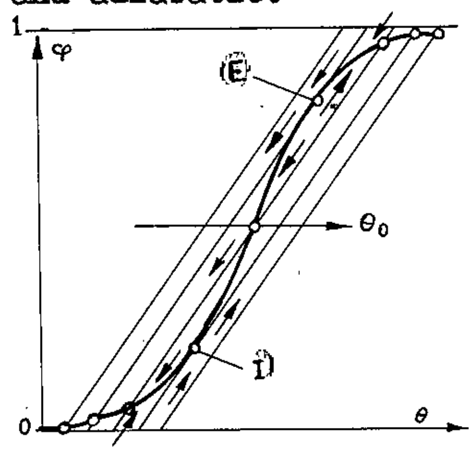

Fig. 3-2. Analysis of the stationary states. (41)

3.7 The heat liberation and the heat elimination curves for kinetic combustion are shown on Fig. 3-2. Both the curves intersect at three points in the φ-θ diagram in the most general case. A possible stationary region corresponds to each of these points. When tangency occurs at one of them, the number of intersection points can be one or two. The upper and lower of the three possible stationary levels of the process are stable. The middle one is unstable and is not realised in practice. The lower level corresponds to negligibly small values of completeness of combustion and to slight heating of the system. The latter is determined on the φ-θ diagram by the difference in values of stationary temperature, θ_{st} (at the point of intersection of the curves) and the initial mixture temperature, θ_o (at the point of intersection of $\varphi_n = \varphi(\theta)$ with the horizontal axis). Physically this region is slow oxidation. The characteristics of the upper stable stationary region are intense heat liberation, high values of completeness of combustion and considerable heating of the system. This is the region of combustion.

3.8 As initial temperature, θ_o increases, the point of intersection moves along the heat liberation curve, $\varphi_I(\theta)$ the stationary values, $\varphi_{st.}$ and $\theta_{st.}$ then increases continuously until the point of tangency, I of the curves $\varphi_I(\theta)$ and $\varphi_{II}(\theta)$ is reached. An infinitesimal rise in temperature would then lead to a sharp increase in the values of $\varphi_{st.}$ and $\theta_{st.}$ and a transition to the upper combustion region. This transition related to an excess of heat liberation over heat elimination is called ignition. A further increase in the value of θ_o is accompanied by a continuous increase in the stationary values, $\varphi_{st.}$ and $\theta_{st.}$; the points of intersection of the curves will slide over the upper branch of the $\varphi_I(\theta)$ curve. As initial mixture temperature decreases, the change at the beginning in $\varphi_{st.}$ and $\theta_{st.}$ will occur smoothly in the combustion region and a continuous decrease is retained until the point of tangency, E of the curves is reached. An infinitesimal decrease in temperature causes a sharp drop in the stationary values, $\varphi_{st.}$ and $\theta_{st.}$ and the transition from upper region to lower. This region leads in practice, to cessation of combustion, i.e., extinction. A further decrease in the parameter, θ_o leads to a continuous decrease of the stationary values of $\varphi_{st.}$ and $\theta_{st.}$

3.9 Hence, both the points, I and E of tangency of heat liberation and heat elimination curves are critical; the lower, I corresponds to ignition and the upper, E to extinction. The critical ignition and extinction conditions do not coincide in the general case. The following inequalities are expressed in relation to the critical ignition and extinction conditions

The value of the initial mixture temperature which leads to ignition in the warming up process is larger than its value corresponding to extinction. In this connection, the curve of the stationary values of completeness of combustion and temperature as shown in Fig. 3-3 has a typical hysteresis character.

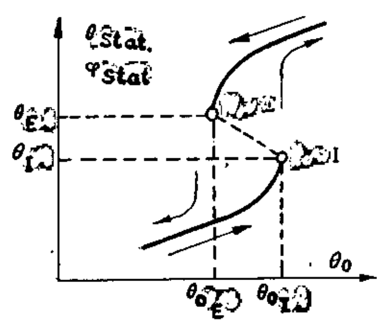

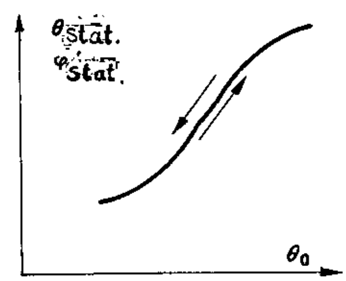

Fig. 3-3. Hysteresis process. Fig. 3-4. Uncritical process.(41)

3.10 A considerably simpler picture ensures for a process where the intersection of the curves $\varphi_I(\theta)$ and $\varphi_{II}(\theta)$ occurs as shown in Fig. 3-4. In this case, the stationary values, $\varphi_{st.}$ and $\theta_{st.}$ always vary continuously as the value of initial temperature, θ_o increases or decreases and the point of intersection is displaced smoothly along the curve, $\varphi_I(\theta)$. Here the critical ignition and extinction phenomena are lacking. This case is uncritical.

3.11 The critical ignition and extinction conditions corresponding to the tangency of heat liberation and heat elimination curves in the φ-θ diagram can be expressed by the following system of equations

$$\varphi_I(\theta) = \varphi_{II}(\theta) \qquad (3\text{-}6)$$

and

$$\frac{d\varphi_I}{d\theta} = \frac{d\varphi_{II}}{d\theta}$$

where $\varphi_I(\theta) = \dfrac{\tau_{SK}}{\tau_{SK} + e^{1/\theta}}$ (3-7)

and $\varphi_{II}(\theta) = \dfrac{\theta - \theta_0}{\nu}$ (3-8)

On simplification, the critical value of the nondimensional temperature is obtained as

$$\theta_{cr} = 1 \pm \sqrt{\frac{1-4\theta_0}{2}} \qquad (3\text{-}9)$$

and the critical value of the co-efficient of completeness of combustion as

$$\varphi_{cr} = 1 - \frac{\theta^2}{\theta - \theta_0} \qquad (3\text{-}10)$$

The minus sign before the radical corresponds to ignition and plus to extinction.

Diffusion Combustion

3.12 Diffusion combustion of cyclone furnaces constitutes two basic component phenomena: delivery of the reacting gas to the surface of the solid phase and the occurrence of chemical reaction thereon. It is assumed that only one chemical reaction occurs between carbon and oxygen on the surface of the solid phase; it is of the first order with respect to concentration of oxygen. In the steady state, the rate of oxygen diffusion to the coal surface equals the rate of reaction at the reacting surface. Elimination of heat from the coal surface is performed solely by convection.

In other words, all the heat being liberated during combustion is absorbed by the combustion products and is carried away from the coal surface.

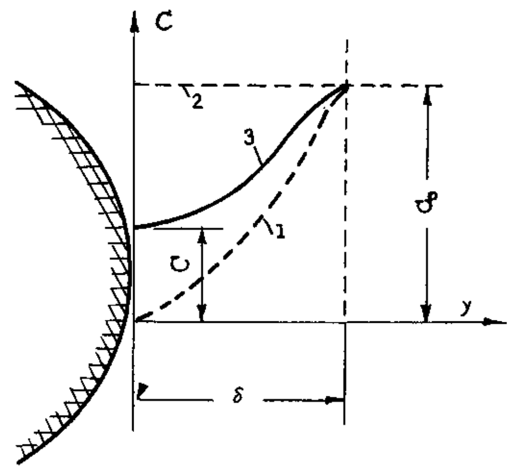

Fig. 3-5. Heterogeneous combustion scheme. 1-Diffusion combustion; 2-kinetic combustion; 3- intermediate case. (41)

3.13 With reference to the reacting coal surface, c_o is the concentration of the reacting gas far from the surface and c is the concentration on the surface itself. The equation of heat liberation is

$$\varphi_I = \frac{\tau_{DK}}{\tau_{DK} + e^{1/\theta}} \qquad (3\text{-}11)$$

and the equation of heat elimination is

$$\varphi_{II} = \frac{\theta - \theta_o}{\nu} \qquad (3\text{-}12)$$

In the stationary regions of the diffusion process, the equality $\varphi_I(\theta) = \varphi_{II}(\theta)$ holds and for determining the critical ignition and extinction points, the following systems of equations are taken into account.

$$\varphi_I(\theta) = \varphi_{II}(\theta) \qquad (3\text{-}13)$$

and

$$\frac{d\varphi_I}{d\theta} = \frac{d\varphi_{II}}{d\theta}$$

3.14 As was shown in the preceding section on kinetic combustion, the graphical solution of the heat balance equation in conformance with the different conditions of $\varphi_I(\theta)$ and $\varphi_{II}(\theta)$ curves intersecting in the $\varphi-\theta$ diagram leads to the possibility of the existance of two kinds of processes, hysteresis and uncritical. Three stationary reaction states are possible, of which the lowest and highest are stable and the middle is unstable and is not realised in practice. The lowest stationary regions corresponds to slight heating of the coal surface and very slow reaction; this region is slow oxidation; the highest region is characterised by high completeness of combustion of the reacting gas and rapid combustion of coal; this is the combustion region.

3.15 In the limiting case, for very high reaction rates ($\tau_K \longrightarrow 0$; $\tau_{sD} \longrightarrow \infty$), the heat liberation curve follows the equation

$$\varphi_I = \frac{1}{1+\tau_{Ds}} = \frac{\tau_s}{\tau_s+\tau_D} \qquad (3\text{-}14)$$

and the heat elimination curve follows the equation

$$\varphi_{II} = \frac{\theta-\theta_0}{\nu} \qquad (3\text{-}15)$$

The equation (3-14) is for purely diffusion combustion with a finite mixture retention time, τ_s in the chamber. This limiting case of diffusion combustion is significant for the high temperature range.

3.16 The curve of the completeness of combustion, $\varphi_I(\theta)$ as function of the nondimensional time, τ_{sD} is shown on Fig.3-6. The completeness of combustion is small values of τ_{sD} i.e., for low stay time or for low diffusion rates; however, the completeness of combustion increases as τ_s increases or τ_D

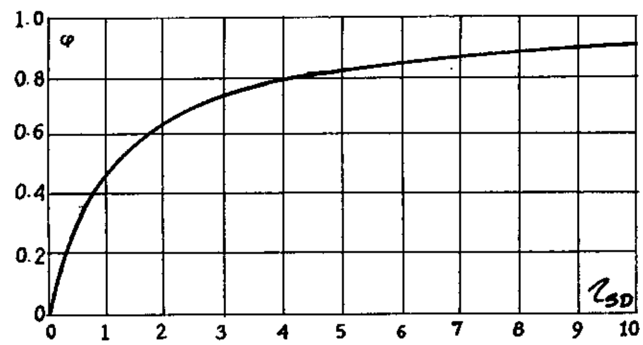

Fig. 3-6. Dependence of completeness of combustion on the nondimensional time for diffusion combustion.(41)

diminishes. The rate of φ is significant in the range of low values of τ_{sD} and very slow for large τ_{sD} .There is, therefore, a particular length of the cylindrical combustion chamber at which the rise of φ is optimum. Any further increase in the chamber length will not result in any appreciable rise of φ .

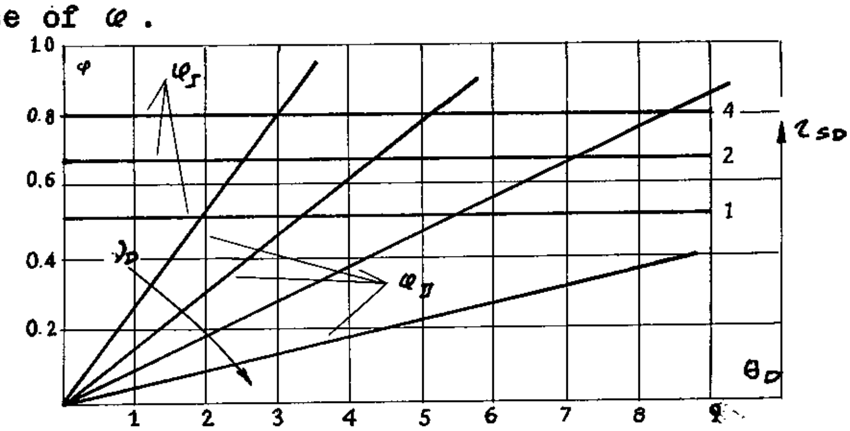

Fig. 3-7. Stationary diffusion combustion region in the plane.

3.17 In order to investigate the steady state combustion region, the heat liberation and the heat elimination curves are shown in Fig. 3-7. Here, the intersection of the lines always occurs at one point. This means that there is just one stationary and stable region in the limiting case of purely diffusion combustion which is characterised by very high values of combustion and heating of the mixture.

GENERAL CASE OF CYCLONE COMBUSTION

3.18 For the general case of cyclone combustion, heat liberation and heat elimination curves follow the equations

$$\varphi_I = \frac{1}{\left(1 + \frac{1}{\tau_{SD}} + \frac{e^{1/\theta}}{\tau_{SK}}\right)} \qquad (3\text{-}16)$$

$$\varphi_{II} = \frac{(\theta - \theta_0)}{\nu} \qquad (3\text{-}17)$$

The expression obtained for the heat liberation curve, $\varphi_I(\theta)$ in the limiting case of $\tau_{SD} \to \infty$ transforms into Eqn. (3-7) for kinetic combustion. In the other limiting case for very high reaction rates, Eqn. (3-16) transforms into Eqn. (3-14) for purely diffusion combustion. The heat liberation curves, $\varphi_I(\theta)$ are shown in the φ-θ diagram on Fig. 3-8. Each group of curves corresponds to one value of τ_{SK}; the nondimensional time, τ_{SD} is the second parameter for the curves within the pencil. The curves, $\varphi_I(\theta)$ are constructed according to the kinetic relationship, Eqn. (3-7) for $\tau_{SD} \to \infty$. The $\varphi_I(\theta)$ curves in the other limiting case $\tau_{DS} \to 0$ depend on the temperature and agree with lines parallel to horizontal axis drawn for diffusion combustion according to Eqn. (3-14).

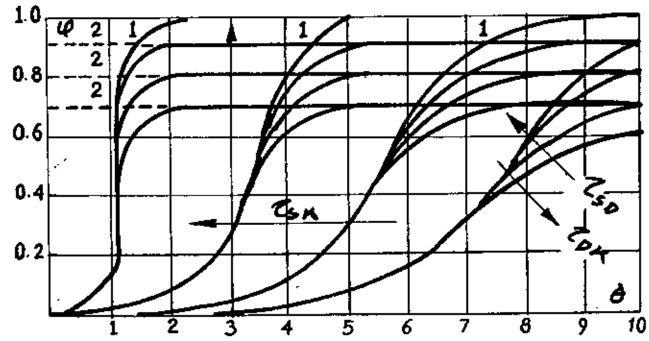

Fig. 3-8. Diagram for the general case. 1- kinetic curves; 2- diffusion curves. (41)

3.19 As is seen from Fig. 3-8, the heat liberation curves, $\varphi_I(\theta)$ practically coincide with the kinetic curves in the beginning on the section of low φ and θ values. As the temperature increases, the curves, $\varphi_I(\theta)$ drawn according to Eqn.

for the intermediate combustion range, deviate all the more for kinetic curves; the deviation starts earlier and becomes greater with the smaller values of τ_{sD} . As the temperature increases further, the $\varphi_I(\theta)$ curve for the general case approximate the diffusion lines for the appropriate τ_{sD} values more and more and then practically coincide. Hence, a kinetic, intermediate and diffusion combustion range (Fig. 3-9) can be isolated approximately for each of the curves for given τ_{sD} and τ_{sK} .

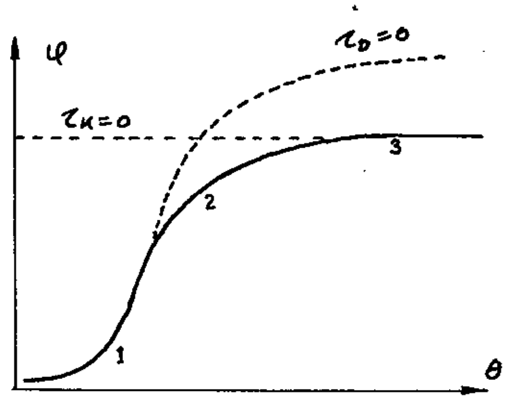

Fig. 3-9. Heat liberation curve, general case. 1-Kinetic; 2-intermediate; 3-diffusion combustion.(41)

3.20 A pencil of heat liberation curves is shown diagramatically on Fig.3-10 for one value of τ_{sK} and several values of τ_{sD} . From the condition of intersection of the heat liberation curves, $\varphi_I(\theta)$ with the heat elimination curves, $\varphi_{II}(\theta)$, the hysteresis process is realised for the four upper curves over a wide variation of θ_o ; curve 1 refers to the uncritical process; curve 2 corresponds to the limiting case where ignition and extinction conditions coincide. The appropriate curves of the stationary values of the temperature are shown on Fig. 3-10b. Here the increased mixing time causes

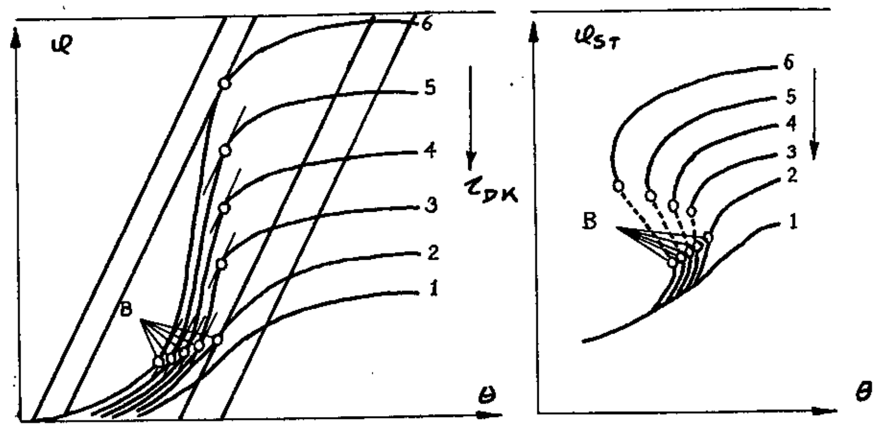

Fig. 3-10. Stationary levels of the process and critical ignition and extinction phenomena for a finite mixing time.(41)

a contraction of the hysteresis loop, an approach in the critical values of φ and θ for the ignition and extinction regions and a transition to the uncritical process for sufficiently large values of τ_D .

3.21 The curves of the stationary values can also be obtained for a variation in the τ_{DK} parameter and for constant θ_o, τ_{bK} and ν . Such a case is shown on Fig. 3-11. A characteristic hysteresis curve of the stationary temperature (Fig.3-11b) is obtained for the heat elimination line 1'-1' on Fig.3-11a and the corresponding continuous stationary temperature curve for the line 2'-2'. In the case of hysteresis process, an increase in the parameter, τ_{DK} leads to a shift in the stationary level to the region of the lower values of the completeness of combustion and temperature of combustion and to extinction; a decrease in τ_{DK} leads to an increase in the stationary values of φ and θ , and to ignition. The critical values of the variable for ignition and extinction are related by the following inequalities:

$$\theta_e > \theta_i \ ; \qquad \varphi_e > \varphi_i$$

and $\tau_{DK_i} < \tau_{DK_e}$.

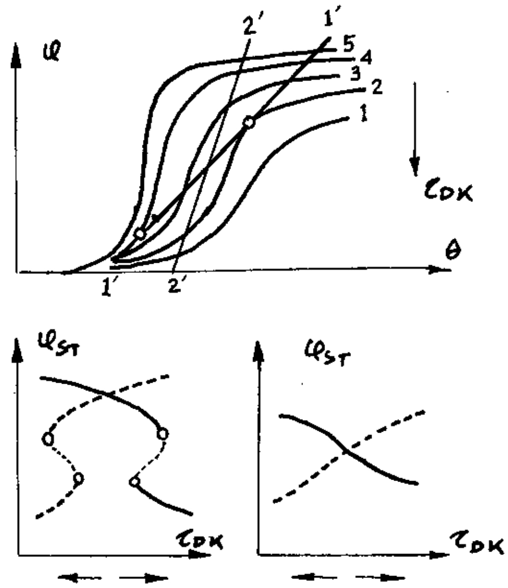

Fig. 3-11. Influence of mixing time on the critical temperature and completeness of combustion.(41)

3.22 The influence of mixing time on the thermal region of the process refers to the solid curves mapped on Fig.3-11b and c. The probable character of the curves of the stationary values of the combustion temperature in the region of the low mixing time values is shown by dashes on the same Fig. 3-11b and c. As regards the character of the curves,it can have two hysteresis loops on both sides of the stable combustion section (Fig.3-12a) or it can drop smoothly on both sides (Fig. 3-12c) or, finally, it can have a hysteresis loop on one side and a continuous temperature deduction on the other (Fig.3-12b and c).

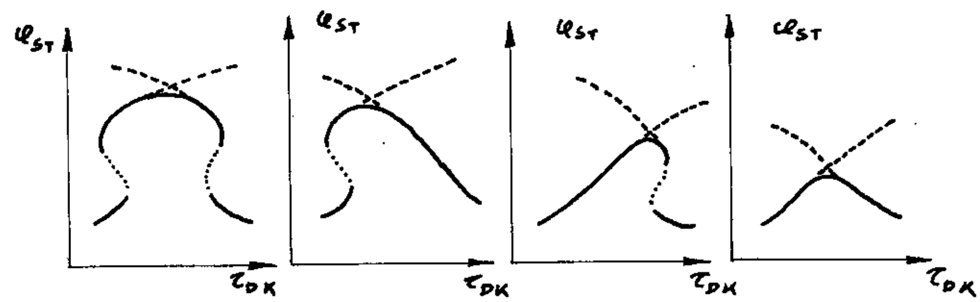

Fig. 3-12. Examples of curves of dependence of the stationary combustion temperature on mixing time.(41)

3.23 The lower stationary levels and approximately the ignition conditions lie in the kinetic combustion region.The extinction conditions for appreciable values of τ_D correspond to a considerably lower completeness of combustion than in the kinetic combustion and to almost to same values of the temperature; extinction in the combustion of a inhomogeneous mixture is always accomplished in the intermediate region. On the whole, an increase in the mixing time, τ_D lowers the stationary values of θ and φ , other conditions being equal, facilitate extinction and makes ignition difficult and, finally, narrows the region where critical phenomena exists. The process makes the transition into the uncritical region for sufficiently large values of τ_D .

3.24 For critical ignition and extinction conditions,we can write,

$$\begin{aligned} \varphi_I(\theta) &= \varphi_{II}(\theta) \\ \frac{d\varphi_I}{d\theta} &= \frac{d\varphi_{II}}{d\theta} \end{aligned} \qquad (3\text{-}18)$$

On simplification,the critical value of the completeness of combustion, φ_{cr} is obtained as

$$\varphi_{cr} = \frac{1 - \frac{\theta^2}{\theta - \theta_0}}{1 + \tau_{DS}} = \frac{\varphi_{cr,Kin}}{1+\tau_{DS}} \qquad (3\text{-}19)$$

where $\varphi_{cr,Kin} = 1 - \frac{\theta^2}{\theta-\theta_0}$.

From $\frac{d\varphi_{cr}}{d\theta} = 0$, the maximum value of φ_{cr} is $(1-2\theta)$ or $(1-4\theta_0)$. In the limiting case where $\theta_0 << \theta$, $\varphi_{cr,Lim} = \frac{1-\theta}{1+\tau_{DS}}$

For kinetic combustion as $\tau_{SD} \rightarrow \infty$, this formula transforms into

$$\varphi_{cr} = 1 - \theta \qquad (3\text{-}20)$$

As τ_D increases, the region where the hysteresis process exists in the $\varphi-\theta$ diagram diminishes more and more in ordinate while remaining invariant along the abscissa. Similarly, the ignition region is also displaced towards lesser values of the completeness of combustion. The line where the ignition and extinction condition coincide is obtained from the inflection conditions of $\varphi_I(\theta)$ curve which is $\frac{d^2\varphi_I}{d\theta^2} = 0$ and is expressed as

$$\varphi_{I=E} = \frac{(\frac{1}{2} - \theta)}{(1+\tau_{DS})} = \frac{\varphi_{I=E,Kin}}{1+\tau_{DS}} \qquad (3\text{-}21)$$

where $\varphi_{I=E,Kin} = (\frac{1}{2} - \theta)$.

This reduction in the region of the hysteresis process for an increase in τ_D and all other parameters constant is illustrated in Fig. 3-13.

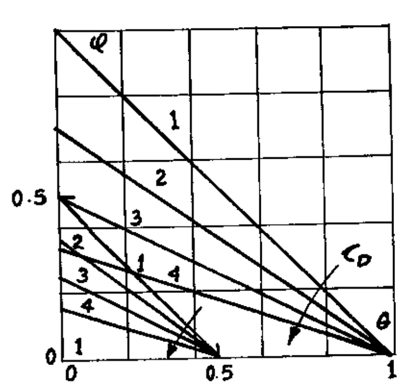

Fig. 3-13. Influence of mixing time on the distribution characteristic regions in the diagram.(41)

3.25 The critical value of the nondimensional temperature is

$$\theta_{cr} = \left[1 + \frac{2\theta_0}{\nu(1+\tau_{DS})} \pm 1 - 4\theta_0 - \sqrt{\frac{4\theta_0^2(1+\tau_{DS})}{\nu}}\right] \Big/ 2\left(1 + \frac{1+\tau_{DS}}{\nu}\right) \qquad (3\text{-}22)$$

The minus sign before the radical corresponds to ignition and plus to extinction. The character of the dependence of θ_{cr} on θ_0 is shown on Fig. 3-14c. The influence of a finite mixing time, τ_D on the critical ignition and extinction conditions which result from Eqn. (3-22) is illustrated diagramatically on Fig. 3-14. They all show that an increase in the mixing time leads to an increase in the region of uncritical process, sometimes to difficult ignition and easy extinction for the total process in the cyclone combustion chamber.

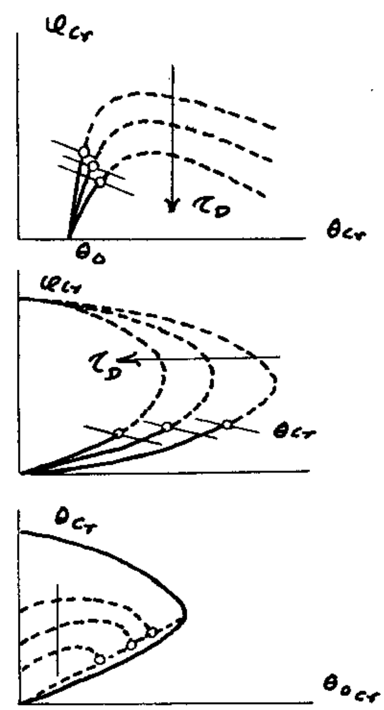

Fig. 3-14. Influence of mixing time on the curves of the critical temperature and completeness of combustion values.(41)

3.26 Earlier, we have stated that cyclone combustion is a heterogeneous process where kinetic and diffusion combustions occur simultaneously. In both kinetic and diffusion combustions, ignition and extinction of the combustible mixture occur under certain defined conditions. The influencing parameters for kinetic combustion are τ_{SK}, θ and ν and those for the diffusion combustion are τ_{DK}, τ_{SK}, θ and ν. Kinetic combustion prevails in regions of low temperature, high air velocities and very small particle sizes whereas diffusion combustion prevails at higher temperature low air velocities and large particle sizes. There are some values of air velocity and temperature at which ignition occurs in the kinetic process of combustion and some other values at which the flame of kinetic combustion dies out and extinction occurs. Similar is the case with the ignition and extinction of diffusion combustion. Since the air velocity and temperature vary widely in the combustion chamber, intermittent transition occurs from one stable state to the other in both the cases. It is anticipated that in the case of our cyclone furnace firing,kinetic combustion will be prevalent in the low temperature region of the furnace i.e., the earlier part of the combustion chamber and diffusion combustion in the region of high temperature,presumably the rear part of the combustion chamber. There are certain limiting values of air velocity, temperature and particle size at which combustion will be stable throughout the whole part of the cyclone combustion chamber. Usually higher air velocities lower temperature and smaller particle sizes initiate the ignition of the kinetic process of cyclone combustion while lower air velocities, higher temperature and larger particle sizes initiate the ignition of the diffusion combustion. A decrease in air velocity, increase in temperature and use of coarser fuel particles leads to extinction in the case of kinetic combustion; on the other-hand, an increase in the air velocity, a decrease in temperature and use of finer fuel particles leads to extinction in diffusion combustion. In the subsequent chapter, we shall study the modeling of cyclone furnace.

CHAPTER IV
MODELING OF CYCLONE COMBUSTION

4.1 Principles of fluid flow dynamics and combustion relating to a cyclone furnace have been enunciated in the previous chapters. Experimentation on a large scale cyclone furnace being too much difficult and expensive, investigation is made on a model cyclone furnace. The reasons for modeling the cyclone furnace are explained together with the advantages and disadvantages of cold and hot combustion models. In the section on principles of modeling, similarity criteria relating to cyclone combustion are presented. Finally, modeling applied to an enclosed jet-combustion which is very similar to the combustion that occurs in a cyclone furnace is illustrated.

4.2 To carry on experiments on a full-size cyclone furnace is enormously expensive of time, money and material. Moreover, cyclone combustion is so complex that eertain desirable measurements are too difficult to make with sufficient accuracy. On the other hand, small scale experiments are comparatively much simpler and also less costly. From practical and economic point of view, we,therefore, make recourse to modeling the cyclone furnace.

4.3 Modeling is a technique of predicting the likely results of one full-scale experiment by interpreting the results of another small scale experiment which is very similar to a large scale experiment. In this case, a small scale experiment is what is ordinarily called a model. Its chief function is to exhibit the effects of change in shape or operating condition more quickly and economically than would be possible by experiments on the full-size prototype. A model should usually satisfy the criteria of geometrical, mechanical, chemical and thermal similarity. Because of a large number of variables being associated with the process of combustion,it is impossible to follow strictly the requirements of similarity theory and as such complete modeling on cyclone combustion is not practicable.

4.4 Combustion models are of two types: hot and cold. Cold model is operated at room temperature and a hot model at the temperature of the prototype furnace. A cold model is sometimes called an isothermal model in which no combustion takes place and also no heat is being added by any energy source. Since a worthwhile study of flow in presence of combustion is very difficult to achieve, hot models are seldom prefered. On the other hand, cold flow studies can be made more readily than hot studies because of absence of fuel factors and offer an obvious advantage in the development of large furnaces where full scale units are expensive and unwieldy to handle. Furthermore, the advantages of cold models are the ease of construction and modification. The measurements may also,be obtained very conveniently with comparatively simpler devices.

4.5 A cold model is capable of giving both qualitative and quantitative information about flow conditions in the prototype furnace.Quantitative data can be obtained on pressure drops and velocity profiles in different parts of the furnace. Qualitative indications are obtainable of turbulence patterns in the furnace gases and regions in which flow impingement or excessive erosion of refractory may occur.

4.6 Cold models are generally operated with either air or water as the working fluid. The kinematic viscosity of the hot furnace gases is of the order of 12 times that of cold air and 130 times that of water. Hence, for dynamic similarity, in a one-twelfth scale model, the cold air velocity should be equal to that in the prototype whereas with water as the working fluid, the velocity is required to be less than one tenth as great. Owing to their lower corresponding velocities,water models are more suitable for visual observation of flow patterns. Air models are easier to construct and more suitable for impingement studies and the determination of velocity profiles by a pitot tube traverse. The type of combustion model and nature of the working fluid chosen largely depend on the nature of investigation that is to be made.

4.7 In the present experimental investigation, a small scale cyclone furnace will be used both as cold and also as hot model; as a cold model, the working fluid will be firstly the air only and subsequently the mixture of air and fuel particles. In the hot model, the working fluid will be the combustion gases. Our objective is to make a qualitative study of cyclone combustion with the hot model and a quantitative estimate with the cold model.

PRINCIPLES OF MODELING

4.8 Similarity criteria of cyclone combustion are discussed from the view point of flow of air and fuel particles,the process of diffusion and chemical reaction.

4.9 Similarity criteria for the flow of fluid within the cyclone combustion chamber are derived from equations of motion, supplemented by dimensional analysis. The fundamental differential equations governing the motion of a viscous fluid are the Navier-Stokes equations. For geometrically similar systems, the equations may be written in the generalised form

$$\frac{\Delta P}{L} = \varphi \left(\frac{\rho v^2}{L}, \frac{\mu v}{L^2}, \rho g \right) \tag{4-1}$$

where ΔP = Pressure drop

L = corresponding linear dimension

v = fluid velocity

ρ, μ = fluid density and viscosity

g = acceleration of gravity

Dividing across by $\frac{\rho v^2}{L}$ and rearranging,

$$\frac{\Delta P}{\rho v^2} = \varphi \left(\frac{\rho v L}{\mu}, \frac{v^2}{L g} \right) \tag{4-2}$$

The group on the left is the pressure coefficient; those on the right are, respectively, the Reynolds number and Froude group.

4.10 Similarity criteria for diffusional processes that occur within the cyclone combustion chamber when fuel burns as it mixes with air are derived from differential equations for mass transfer with forced convection which are the Navier-Stokes equations together with mass transfer equations. For geometrically similar systems,the equations may be written in the generalised form,

$$\frac{KL}{\mathcal{D}} = \varphi\left(\frac{\rho v L}{\mu}, \frac{\mu}{\rho \mathcal{D}}\right) \qquad (4\text{-}3)$$

where K = mass transfer coefficient

$\mathcal{D}$ = diffusion coefficient.

The groups $\frac{KL}{\mathcal{D}}$, $\frac{\rho v L}{\mu}$ and $\frac{\mu}{\rho \mathcal{D}}$ are the Sherwood, Reynolds, and Schimdt or Colburn groups respectively.

4.11 In connection with the process of diffusion in cyclone combustion, two more dimensionless groups are also significant. One is the Lewis or Lewis-Semenov number which is the ratio of the energy transported by conduction to that transported by diffusion; viz., $N_{Le} = \frac{K}{\rho \mathcal{D} c_p}$ in a binary mixture as is the case with the cyclone furnace. It is apparent that where the Prandtl number, N_{Pr} is a rough measure of the relative importance of momentum transfer and heat transfer while the Schimdt number, N_{Sc}, is a rough measure of the relative importance of momentum transfer and mass transfer. As in the case of Prandtl number Schimdt number is often somewhat less than unity. In many systems, Lewis number is very nearly unity; it is often slightly less than unity in combustible mixtures. The approximation Lewis number, N_{Le} = 1, is frequently very helpful in the combustion analysis.

4.12 Another is the mass transfer number. The differential equation for molecular diffusion in a fluid in steady motion is

$$\mathcal{D}\left(\frac{\partial^2 m_j}{\partial x^2} + \frac{\partial^2 m_j}{\partial y^2} + \frac{\partial^2 m_j}{\partial z^2}\right) - u\frac{\partial m_j}{\partial x} - v\frac{\partial m_j}{\partial y} - w\frac{\partial m_j}{\partial z} = 0 \qquad (4\text{-}4)$$

where x,y,z are rectangular space co-ordiantes

u,v,w are the velocities of the fluid in x,y,z directions.

The equation(4-4) expresses the fact that the net rate of diffusion of the substance, j into unit volume is exactly equal to the net rate at which it is convected out. If the flow pattern remains constant, the mass transfer rate is directly proportional to concentration difference. Mass transfer rate at the surface is equal to density times the normal velocity. The component j is actually being transferred in two ways by convection and by diffusion. Introducing a new variable

$$b = \frac{m_j}{(m_{j_s} - 1)}$$

where s refers to the surface,

The differential equation for mass transfer can be transformed by dividing Eqn. (4-4) by $(m_{j_s} - 1)$ into

$$\mathcal{D}\left(\frac{\partial^2 b}{\partial x^2} + \frac{\partial^2 b}{\partial y^2} + \frac{\partial^2 b}{\partial z^2}\right) - u\frac{\partial b}{\partial x} - v\frac{\partial b}{\partial y} - w\frac{\partial b}{\partial z} = 0 \qquad (4\text{-}5)$$

'b' is here essentially negative, since m_j is always positive but less than one. Eqn. (4-5) may be regarded as the equation governing the diffusion of some property,'b' in the fluid which is such that when unit quantity of 'b' diffuses out of the stream, unit mass of the transferred substance enters it. The mass transfer rate depends on the difference in the values of the variable in the gas stream and at the surface. The difference occurs so frequently that it is better to denote it by $B = b_g - b_s$ and call it by mass-transfer number. It is the driving force for mass transfer in dimensionless form. When B is positive, mass transfer is outwards from the surface; when B is negative, mass transfer is inwards. A transfer number less in value than - 1 is impossible because no matter can leave the fluid stream than is initially present there. B = - 1 when a pure fluid is fully absorbed.

4.13 A chemical regime prevails when the over-all rate of change is controlled by a chemical reaction velocity, which consequently appears in one or more of the dimensionless criteria. For a continuous-flow system Damkohler proposed five dimensionless criteria,

$$\frac{UL}{cv} = \varphi\left(\frac{UL^2}{c\mathcal{D}}, \frac{qUL}{c_p \rho T v}, \frac{qUL^2}{KT}, \frac{\rho v L}{\mu}\right). \qquad (4-6)$$

where U = reaction rate expressed as moles of reactant A which react per unit volume and time

c = concentration of reactant A per unit volume

$\mathcal{D}$ = diffusion coefficient of A

q = heat generated per mole of A reacting

c_p, ρ, K, μ = specific heat at constant pressure, density, thermal conductivity and viscosity of reaction mixture, respectively

T = temperature of reaction mixture

v = linear velocity of reaction mixture

L = linear dimension.

Damkohler's dimensionless terms may be transformed into more customary groups, eliminating U from the right hand side of the equation, (4-6).

$$\frac{UL}{cv} = \varphi\left(\frac{\mu}{\rho\mathcal{D}}, \frac{qc}{c_p \rho T}, \frac{c_p \mu}{K}, \frac{\rho v L}{\mu}\right) \qquad (4-7)$$

Thus, the chemical reaction velocity group on the left is a function of the Schimdt, Prandtl and Reynolds numbers and a group containing an entropy term. The equation (4-7) neglects the effect of heat transfer by radiation. Many chemical reactions occur at temperatures such that radiation is an important if not the predominant mode of heat transfer so that a complete generalised equation should include

Thring's radiation gboup and the ratio of absolute temperature. The full equation then becomes

$$\frac{UL}{C\nu} = \varphi\left(\frac{\mu}{\rho D}, \frac{qC}{C_p \rho T}, \frac{C_p \mu}{k}, \frac{\rho C_p \nu}{\sigma e T^3}, \frac{T}{T_r}, \frac{\rho \nu L}{\mu}\right) \quad (4\text{-}8)$$

This is the generalised equation for a continuous flow chemically reacting system.

4.14 Assuming mass transfer by molecular diffusion to be negligible compared with transport by eddy diffusion and bulk flow, the Schimdt group may be neglected. It is often permissible to disregard the Reynolds number, i.e.; to assume that the flow pattern does not significantly influence the chemical reaction. The transverse temperature gradients inside the reacting system are negligible compared with the gradient through the wall of the reaction vessel. In practice, the heat flux per unit area of reaction vessel wall, H_W can be artificially varied by devices such as insulation, jacketing or electrical heating of the reaction vessel. It is, therefore, an independent variable and the Prandtl and radiation groups together with the ratio of absolute temperatures may be replaced by a single group, $\frac{q\nu L}{H_w}$, representing the ratio of heat generated by heat lost or gained through the vessel walls. It is again convenient to eliminate U by dividing by $\frac{UL}{C\nu}$, whereby the group becomes $\frac{qC\nu}{H_w}$. Hence, the generalised equation for chemical similarity becomes

$$\frac{UL}{C\nu} = \varphi\left(\frac{qC}{C_p \rho T}, \frac{qC\nu}{H_w}\right) \quad (4\text{-}9)$$

Modeling applied to an Enclosed Jet

4.15 Cyclone combustion is very similar to the combustion of a jet of combustible mixtures in an enclosed cylindrical space. Here modeling applied to such a case is illustrated.

4.16 A horizontal cylindrical furnace is heated by a jet of fuel particles issuing from a nozzle and meets a separate stream of air inside the combustion chamber, the burnt gases

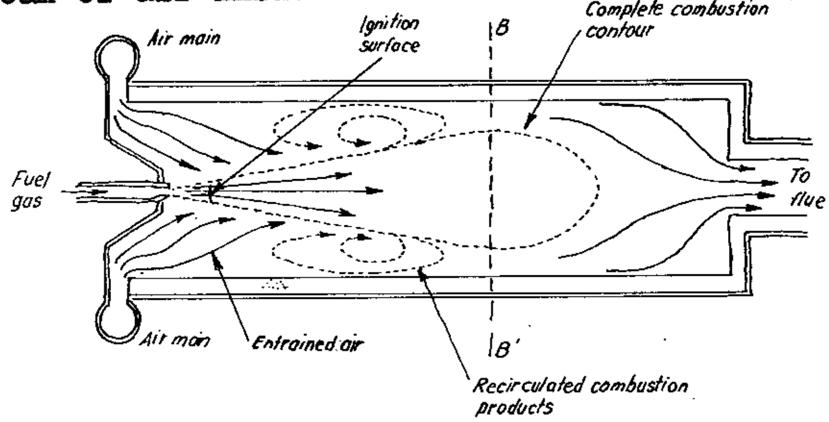

Fig. 4-1. Internal circulation and flame contour in a furnace

flow out as the flue gas. Let

N = actual mass ratio of (air + fuel)/fuel

N_o = Stoichiometric mass ratio of (air + fuel)/fuel

(percentage excess of air = 100(N-No)/ (N_o -1)

v_{fg} = mean velocity of the burnt gases in region where the temperature has become uniform and equal to T_f

ρ_{fg}, μ_{fg} = density and viscosity of burnt gases at temperatures T_f

L = linear dimension along the combustion chamber

N and N_o are ready- made dimensionless similarity criteria. The first governs the relative mass flow rates in the burner nozzle and combustion chamber; the second fixes the percentage excess air and hence the mixing length for a given value of N. (instead of N_o the excess air ratio could be taken as one criterion.). The flow pattern in the latter stages of combustion and afterward is fixed by the Reynolds number and hence $\frac{\rho_{fg} v_{fg} L}{\mu_{fg}}$ constitutes a third criterion.

4.17 The flow pattern in a furnace is complicated by the large rise in temperature of the gases in the first part of the combustion chamber near the burner nozzle. In this region, the jet of the fuel gas is expanding as it entrains combustion air, mixes with it, and burns. The temperature across the flow path is far from uniform and the concept of a mean velocity has no application, since the flow consists of a high velocity jet surrounded by relatively stagnant air. Thus, equality of Reynolds number in the latter stages of combustion is no criterion of similarity in the early stages, and it is conditions in the early stages that largely determine the shape and size of the flame.

4.18 Thring and Newby (36) derived a similarity criterion for the early part of the flame by assuming conservation of momentum in the free jet region, before the expanding jet impinges on the combustion chamber walls. A free jet of fluid of density, ρ_o which entrains a surrounding fluid of density ρ_s is being considered. Except very close to the nozzle, the velocity profile across a free jet is constant, so that one can write

$$\rho_{rx} = \rho_x \; \phi_1(\eta)$$

$$u_{rx} = u_x \; \phi_2(\eta)$$

where x = distance along axis of jet from an imaginary point source at apex.

r = radial distance of a point P from axis of jet at distance x

ρ_{rx} = density of mixture at P

ρ_x = density of mixture on axis of jet at distance x

u_x = local velocity of mixture on axis of jet at x

u_{rx} = local velocity of mixture at P

η = r/x

Let G = jet momentum, defined as mass rate of flow of fluid times velocity.

4.19 It is assumed that the surrounding fluid enters at a negligible velocity so that all the momentum of the expanding jet is derived from the momentum of the nozzle fluid, and that this remains constant over free-jet region.

4.20 The jet momentum across an annular element of radius r and width dr is given by

$$G_r = 2 u_{rx}^2 \rho_{rx} \pi r dr$$

If r_e is the radius to the edge of the jet, the total jet momentum across the plane x is

$$G = u_x^2 \rho_x \pi x^2 K_{12}$$

where $K_{12} = 2 \int_0^{\eta_e} \varphi_1(\eta) \varphi_2^2(\eta) \eta \, d\eta$,which is independent of x. Hence,

$$u_x = \sqrt{\frac{G}{\rho_x x^2}} \sqrt{\frac{1}{\pi K_{12}}} \tag{4-10}$$

Similarly, the total mass flow of the jet is given by

$$M = u_x \rho_x \pi x^2 K_{11}$$

where $K_{11} = 2\int_0^{\eta_e} u_1(\eta)\, u_2(\eta)\, \eta\, d\eta$, also independent of x. Substituting for u_x from Eqn. (4-10)

$$M = x\sqrt{G\rho_x}\sqrt{\frac{\pi K_{11}^2}{K_{12}}}$$

or

$$\frac{M}{x} = \sqrt{G\rho_x}\; K_3$$

4.21 The original jet of density, ρ_o soon entrains many times its own mass of the surrounding air and rapidly heats up. Hence the density ρ_x at the axis of the jet soon approximates to the density ρ_{fg} of the final combustion gases at flame temperature. Thus, to a reasonable approximation one may write

$$\frac{M}{x} = \sqrt{G\rho_{fg}}\; K_3 \qquad (4\text{-}11)$$

where K_3 is a constant depending only upon the jet angle, which in turn depends upon the nozzle geometry.

4.22 From Eqn.(4-11), the total mass flow of original nozzle fluid plus entrained fluid at distance L from the origin is

$$M = K_3\sqrt{G\rho_{fg}}\; L$$

If a = cross sectional area of the jet nozzle

M_o = mass-flow rate of nozzle fluid.

the mean velocity at the nozzle is $\frac{M_o}{\rho_o a}$, and since G is constant,

$$M_o = \sqrt{G\rho_o a}$$

Hence, the ratio of the total jet fluid to nozzle fluid at length of travel L is

$$\frac{M}{M_o} = K_3\frac{L}{\sqrt{a}}\sqrt{\frac{\rho_{fg}}{\rho_a}} \qquad (4\text{-}12)$$

K_3 being a geometrical constant.

$\frac{dP}{dx}$

4.23 Equation (4–12) gives the fourth dimensionless criterion affecting the geometry of the flame. Putting l/L as a shape factor, the complete generalised dimensionless equation for the enclosed jet combustion is

$$\frac{l}{L} = u\left(N, N_o, \frac{\rho_{fo} v_{fo} L}{\mu_{fo}}, \frac{L^2 \rho_{fo}}{a \rho_o}\right) \qquad (4\text{-}13)$$

4.24 In most industrial furnaces, the Reynolds number is of the order of 100,000 and in this range a considerable variation has little influence on the flow pattern. For example, a model furnace may be operated at Reynolds number as low as one-tenth those in the prototype without sensibly impairing the similarity of flame contours. Hence, in practice the Reynolds criterion may be neglected, and Eqn. (4–13) becomes

$$\frac{l}{L} = u\left(N, N_o, \frac{L^2 \rho_f}{a \rho_o}\right) \qquad (4\text{-}14)$$

Assuming constant values of N and N_o, this gives the scale equation

$$a = \frac{L^2 \rho_f}{\rho_o} \qquad (4\text{-}14a)$$

4.25 Equation (4–14a) shows that the two geometrically similar furnaces in which the fuel and flame temperatures are different will not give similar flame contours unless the scale of the burner nozzles differs from that of the combustion chambers. Where the flame contour in a prototype furnace is to be predicted by means of the cold-air model, then the scale of the model burner nozzle must be changed still more. If ρ_a be the density of air used as both nozzle fluid and surrounding fluid in the model and ρ_o', ρ_f' be the densities of nozzle fluid and combustion gases in the prototype then $\rho_f = \frac{\rho_f'}{\rho_a}$ and $\rho_o = \frac{\rho_o'}{\rho_a}$ .Equation(4–14a) thus becomes

$$a = \frac{L^2 \rho_f'}{\rho_o} \qquad (4\text{-}14b)$$

4.26 We summarise that a model is a small scale experiment, usually constructed for predicting the performances of a large experiment which involves more complicacy and cost. Hot and cold models are generally used for combustion modeling. In the case of cyclone combustion, we shall use a small scale cyclone furnace as cold model using air and as a hot model using combustion gases by burning the mixture of air and fuel particles. We mainly concentrate on the modeling of cyclone furnace from the fluid mechanical standpoint. Similarity criteria that are to be satisfied for the fluid regime are the pressure coefficient, the Reynolds number and the Froudes group. If Reynolds number is sufficiently large, the Reynolds numbers of model and prototype need not be equal. Similarly, if the Froudes group is sufficiently large as is the case with high velocity flows, the Froudes groups of model and prototype need not be equal. If the flows have low Froude number, this rule cannot be safely ignored. Since we are using the same fluid in the cold model and prototype furnaces, the flow pattern in both the cases will be similar. In the hot model the operating temperature will be the same as in the prototype furnace. In otherwords, the model and prototype furnaces will have similar temperature profiles. Geometrical similarity will be maintained both in the case of hot and cold models. While geometrical similarity is usually required between model and prototype in all gross features of the small scale apparatus, minor departures from similarity are permissible and may even be advantageous. To have the similar flame contours in model

and prototype furnaces, the nozzle and the combustion chambers should obey the scale equation, $a = \frac{L^2 g_f'}{g_o}$
In the following chapter, we shall describe the experimental set-up of the cyclone furnace.

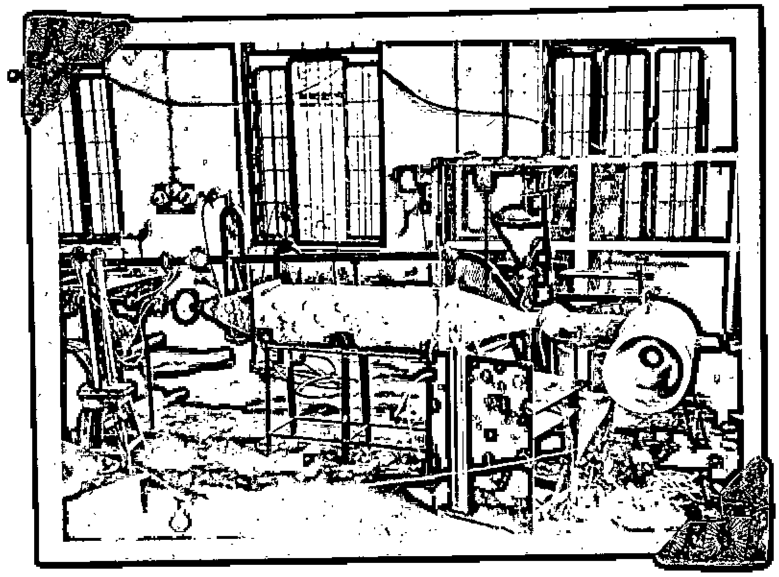

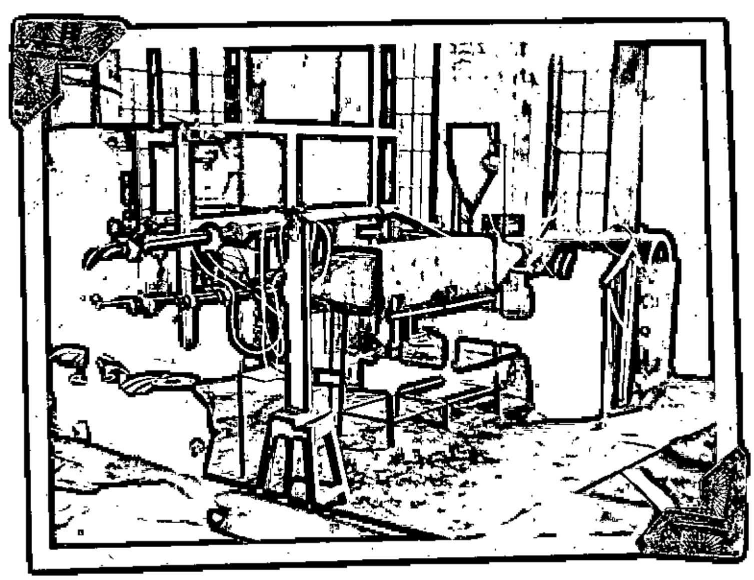

CHAPTER V

EXPERIMENTAL METHOD

EXPERIMENTAL SET-UP

5.1 The experimental set-up for the cyclone furnace consisted primarily of an air blower, an air heater, a gravity-controlled fuel-feeding hopper and a horizontally placed cylindrical combustion chamber fitted with nozzles for admitting air and pulverised fuel. The schematic diagram of the experimental set-up is shown on Fig. 5-1.

5.2 The blower was run by a 3-hp capacitor motor with an A.C. supply of 220 volts. The blower took air from the atmosphere through a 3 in-suction pipe. The delivery end of the blower was connected with 2 in- C.I. pipe which went upto a height of 37 inches above the floor level and then branched into two. One constituted the primary air line and the other the secondary air line. Primary air carrying the fuel particles from the hopper entered the combustion chamber through a nozzle. Secondary air being heated in the electric heater entered the combustion chamber through another nozzle.

5.3 Secondary air was heated by a 21 Kw heater. The air heater was a 4 ft x 1 ft x 1 ft rectangular duct with two conical sections at the two ends minimising the pressure losses due to sudden expansion and contraction. The heater was made out of 1/16 in M.S. plate. To minimise heat loss, the inside space of the heater was covered with 3/16 in. asbestos sheet and the outside was covered with a layer of paste made from

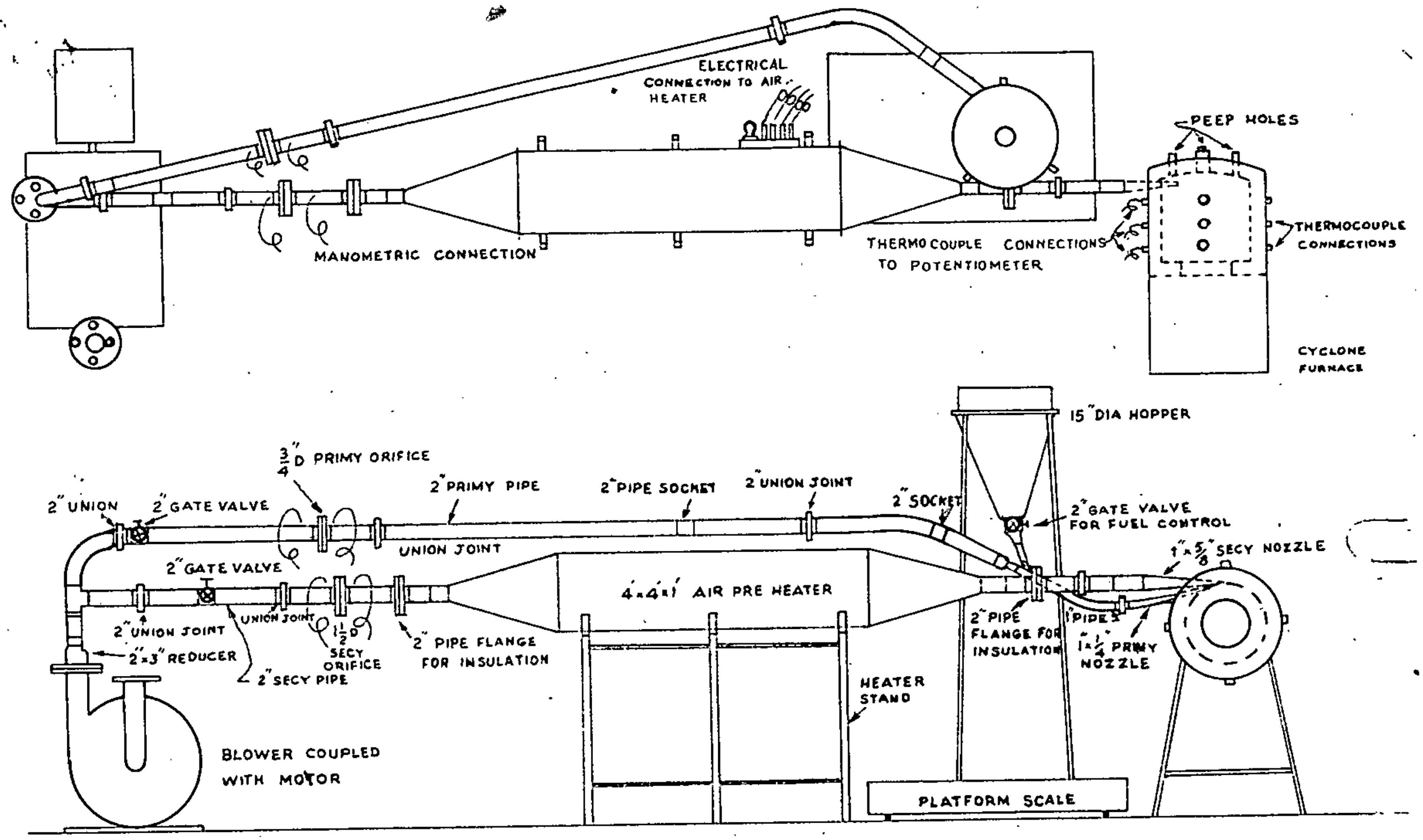

Fig:-5·1 Schematic Sketch of the Experimental Set-up of the Horizontal Cyclone Furnace.

asbestos powder and fire clay. Nine 2 Kw and three 1 Kw heating coils were wound on twelve porcelain tubes (3/4 in. diameter, 1 ft long) which were held vertical inside the rectangular duct by inserting bolts through the tubes and fastening the bolts with the M.S. plate by the nuts. The heating coils were connected through a switch to an Electric supply. The air heater as a whole was electrically insulated from the rest of the experimental set-up by flange coupling wrapped with ampere tapes. To detect any short circuit in the electrical connections to the heater, an electric bulb was fitted in series with the body of the heater and the earth.

5.4 The cross section at the tip of the nozzle, through which primary air carrying the fuel particles entered the combustion chamber, was rectangular(1 in x 1/4 in). The nozzle for admitting the primary air and the fuel particles was connected with a one in-C.I. pipe. The nozzle for admitting the secondary air had also a rectangular cross section(1 in x 5/8 in).at its tip. It was connected with a 2 in-C.I.pipe. The two nozzles were so positioned that the primary air carrying the fuel particles and the secondary air entered the combustion chamber tangentially.

5.5 Fuel-feeding system consisted of a hopper vertically placed on a trippd stand resting on a platform scale. The diameter of the hopper was 15 in. at the top and 1-1/2 in at the bottom. The hopper was connected with a one in pipe line through a 1-1/2 in. gate valve. The connection was made flexible with 1-1/4 in. leather impregnated rubber pipe.

5.6 The cyclone combustion chamber was essentially a horizontal cylinder. The major part constituted the primary combustion chamber and the remaining the secondary conbustion chamber. The two chambers were separated by a disc having a central hole of 6 in. diameter. The furnace shell (17 in. diameter, 33 in. long) was made out of 1/8 in M.S. plate. It was insulated with a mixture of fire clay and asbestos powder. The insulation thickness was 2.5 in.The primary combustion chamber was 12 in. in diameter and 18 in. long. There was a hole (1-1/2 in x 1-1/2 in) at the bottom near the end of the primary combustion chamber for the removal of molten ash(slag). There were three inespection holes (2 in. diameter) at the front end of the primary combustion chamber. The central inespection hole was also used for introducing the gas flame for preheating the primary combustion chamber. The furnace was supported on a steel frame.

5.7 The arrangement for preheating the primary combustion chamber consisted of a gas torch,one cylinder filled with oxygen, one cylinder filled with acetylene, flow meters and pressure regulators connected with the cylinders.

INSTRUMENTATION

5.8 A circular orifice of 3/4 in diameter was installed between two flanges connected with 2 in primary air pipe line. The pressure tappings were connected to a U-tube differential manometer containing water. Another orifice of 1-1/2 in. diameter was installed similarly in the secondary air pipe line. Two in. globe valves situated upstream from the orifice controlled the amount of air flow through the primary and secondary pipe line.

5.9 To measure the temperature of the hot secondary air, before it entered the combustion chamber, a chromel-alumel thermocouple was inserted in 2 in pipe line just after the air heater. Another twelve such thermocouples were installed at three different sections of the furnace. At every section there were four thermocouples, equally spaced around the periphery of the chamber. The cold junctions of all the thermocouples were connected with a potentiometer through a rotary switch. The thermocouples were calibrated following standard procedures.

5.10 To measure the velocity at different sections and at different height, three graduated pitot tubes were installed on the furnace top at three different sections. One pitot tube was near the nozzle, the second near the throat and the third in between the throat and the nozzle. A fixture was also made to traverse the velocity probe horizontally along the length of the furnace. These four pitot tubes were connected with draft gages. A pitot tube connected with a U-tube differential manometer containing water was used to measure the velocity of primary and secondary air at the tip of the nozzles.

5.11 The flow of the fuel particles from the hopper into the primary line was controlled by a gate valve. The amount of fuel, carried by primary air inside the furnace was measured with a platform scale.

5.12 Platinum-Platinum-Rhodium thermocouple was made for measuring the temperature of the furnace. Optical pyrometer was also used to measure the temperature of the flame.

TEST PROCEDURE

5.13 Two sets of experiments were carried out; one set was performed without firing the furnace but with the flow of air and fuel particles into the furnace and the other set was carried out during the combustion.

5.14 During every run, the blower was started by switching on the starter of the capacitor motor. The primary and secondary air flows were adjusted to the desired range by controlling the globe valve. Velocity probes were traversed vertically and horizontally inside the furnace.The readings were recorded from the draft gages. The nozzle velocities were also measured by the pitot tubes attached with the U-tube manometer. While measuring the velocity of primary air at the tip of the nozzle,secondary air supply was totally stopped and similarly, the primary air flow was stopped while measuring the velocity of secondary air at the tip of the nozzle.

5.15 The secondary air was then heated in the air heater to different temperatures using separately single phase,two phase and three phase A.C. supply. The temperature distribution along the length of the combustion chamber and also across its sections were studied with the thermocouples. With the supply of primary air and secondary air into the combustion chamber, pitot tubes were traversed vertically and horizontally and deflections of the inclined gages were recorded.

The velocity of hot secondary air at the tip of the nozzle was also measured.

5.16 Samples of pulverised fuel were prepared with the standard sieves. Each of the sample was fed into the primary line. The necessary flow of primary air for carrying the fuel uniformly into the furnace was determined for every size of fuel particles. The fuel rate (lb/hr) was also recorded for different amounts of primary air flow.

5.17 Before the furnace was fired, the supply of air through the nozzles, the supply of fuel particles into the primary line and the electric supply to the air heater were checked. The air heater was then given electric supply. Simultaneously, the gas torch was lighted by the jet of oxygen and acetylene gases and the flame was put inside the furnace through the central inspection hole. The heating was continued for about an hour. During traversing the gas flame, the throat of the furnace was kept almost closed by the fire bricks to ensure uniform heating of the furnace.When the furnace was red hot,the blower was started. With the admission of primary and secondary air, temperature of the furnace dropped and the furnace became dull red. Heating was continued till the inside of the furnace was again red hot. The fuel was then supplied and onset of ignition was carefully observed. The fire bricks, placed at the throat of the furnace were removed. The ignition temperature was recorded by Pt.-Pt-Rh. thermocouple. If ignition did not occur, fuel supply was cut off and flame heating was continued.

5.18 The flow of secondary air was varied very slowly. The effect of secondary air flow on the stability of combustion flame was carefully studied. The temperatures and the velocities at which flame became stable and also at which the flame died out completely were recorded. While varying the secondary air flow, Pt. Pt-Rh thermocouple was traversed along the length of the furnace and the temperatures at different sections of the furnace were recorded.When the flame became stable,the distance of the flame from the nozzle section was measured.

5.19 When all the observations were recorded,the fuel supply was cut off. The air heater was then switched off. The flow of the primary and the secondary air was increased to remove the fuel particles from the system and also to cool the heater and the combustion chamber. The blower was run for about fifteen minutes,after the fuel supply was stopped. Finally, the blower motor was switched off.

5.20 The above sequence of observations were followed while firing the cyclone furnace with every size of pulverized fuel.

PRECAUTIONS TAKEN

5.21 (i) Air leakages through the joints of the pipe line were rectified.

(ii) The experimental set-up was tested for electrical insulation and any short circuit in the electrical connections.

(iii) During preheating the furnace, the gas flame was traversed uniformly inside the combustion chamber.

(iv) To safeguard against any fire hazard,fire extinguisher was kept near the firing place.

CHAPTER VI

RESULTS

6.1 In the present experimental investigation, the small horizontal cyclone combustion chamber was used as air models and prototype furnace. Investigation was divided into two phases. During the first phase, experiments were performed without firing the furnace but with the flow of air and fuel particles. During this phase the cyclone furnace was used as cold air and hot air models. In the second phase of this work, the cyclone combustion chamber was used as a prototype furnace and the effect of flow and size of the fuel particles on the process of cyclone combustion were studied. The furnace was fired with fuel particles of different fineness. The experimental data and tabulated results are presented in the appendix A. The graphical plots of the results are presented in this chapter.

6.2 During the first phase of the present investigation the cyclone combustion chamber was used as a cold air model. With tangential admission of primary air and secondary air into the cyclone chamber, the flow pattern inside the combustion chamber was studied. The primary air flow was kept constant and secondary air varied. The pitot tubes were traversed at three different sections of the furnace to study the axial velocity pattern. Table I shows the draft gage readings for traversing velocity probes. Figure 6-1 illustrates the axial velocity pattern inside the cyclone chamber at its different sections for 1.5 in. primary orifice manometer deflection and 9" secondary orifice manometer deflection. For other quantities of secondary air it appears from table XV that the readings are similar. So only one graph has been shown.

6.3 Table III shows the static pressure variation at different sections of the cyclone chamber used as cold air model. Here also the primary air flow was kept constant and secondary air flow was varied. Static pressure of air before the nozzles and static pressure at the four points at different section of the cyclone chamber were measured by static pressure probes. From the readings given in table III it seemed clear that the maximum pressure loss occurred at the nozzle.

6.4 On heating the secondary air in the electric preheater upto a temperature of about 500°F before it entered the combustion chamber, the cyclone chamber was used as a hot air model with the hot air model axial flow velocity, static pressures and temperature distribution were studied. As before, primary air flow was kept constant and secondary air flow varied. The results of the pitot tube traverses, static probe traverses and thermocouples traverses have been presented in Table VII, VII, VIII & IX. Table XV shows that the axial velocity is greater at the surface and very small near the center. The magnitudes of axial velocities were higher than the previous ones. Figure 6-2 illustrates the axial velocity profiles for hot air at sections A, B and C of the combustion space. Since from Tables XV & XVI it appears quite clear that the trend of curve will be more or less similar. Table XV gives the static pressure at the region before the nozzle and also the static pressure distribution inside the cyclone furnace. Here also it was found that maximum pressure loss was at the nozzle point.

6.5 Thermocouples were traversed along the length and also along the radius of the cyclone combustion chamber with hot air as the working fluid. Table I x gives the temperature distribution of hot air at section A, B and C of the furnace along its radius. The chamber surface temperature was quite higher than that of its centre. Table I x shows the radial temperature distribution of hot air model. The emf readings obtained from the potentiometer were corrected accordingly for the cold junction temperature as room temperature. The correction factor and temperature values were taken from hand book of physics by Weast (44). Figure represents the temperature distribution along its length. There was a drop in temperature of air as it moved towards the throat. Different ~~ats~~ sets of readings were obtained for constant primary air flow and varying amount of secondary air flow. Since the readings for all the sets were similar the radial temperature distribution and temperature distribution along the length in the cyclone chamber of hot air model were shown for a particular flow of secondary air in figures.

6.6 As a prototype furnace, studies were undertaken to determine the satisfactory conditions for the transport of fuel particles in suspension in primary air into the combustion chamber. It was seen that a particular optimum value of primary air was necessary for carrying the fuel particles of a certain furnaces. Figure 6-3 illustrates this phenomenon. For coarser fuels primary air velocity was higher and for finer fuels comparatively smaller. From table X it is also clear that the fuel rate is optimum for a particular size of fuel particles because of the satisfactory transport condition relating to primary air flow, fuel valve opening and size of the fuel particles. Transport of fuel particles finer than 100-mesh and coarser than 8-mesh were not possible with the fuel feeding mechanism of the present experimental set up.

6.7 The prototype furnace was fired with crushed peat coal of size ranging from 8-mesh to 100-mesh. The effect of secondary air velocity and size of the fuel particles on the process of cyclone combustion, specially on the phenomena of ignition and extinction were studied. The results of the performances during combustion in the prototype furnace are summarised in table XIV . The temperature distribution along the length and also the radius of the prototype furnace during combustion have also been studied. During every run, the secondary air temperature was kept constant, the primary air flow was also fixed before hand for a particular size of the fuel particles. Secondary air flow was only varied. Figure 6-11 illustrates the temperature distribution along the radius at sections A, B and C of the prototype furnace. The chamber surface temperatures were much higher then temperature at the centre. Figure 6-12 also shows the temperature distribution along the length of the combustion chamber of the prototype furnace. Although the temperature profiles followed the similar trend, there was some deviations also because of extra turbulence and radiative heat transfer during combustion.

6.8 Figure 6-9 shows the ignition and extinction temperature for different size of fuel particles. The values of primary air flow and secondary air flow were not same for all sizes of fuel particles. The curve showing the ignition temperature versus fuel size was regular. But the other curve showing the extinction temperature was some what peculiar. Nevertheless, it was observed that temperature of extinction was higher than igntion temperature.

6.9 Figure 6-7 illustrates the secondary air flow necessary for maintaining stable combustion and also for extinction. With the decrease in fineness of the size of fuel particles more secondary air velocity was necessary for sustaining the flame of combustion.

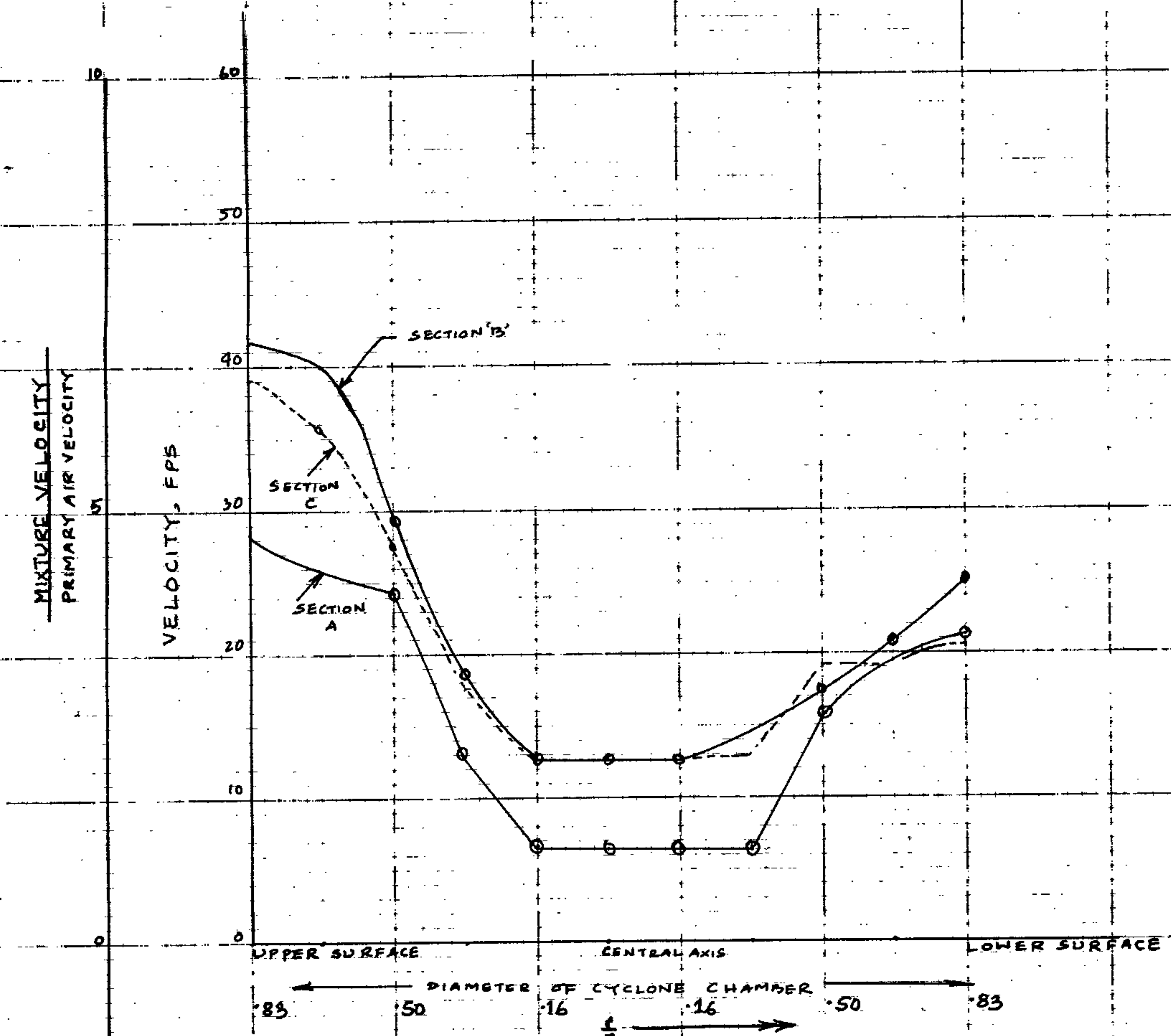

Fig. 6-2. AXIAL VELOCITY DISTRIBUTION OF AIR IN THE CYCLONE CHAMBER OF ~~HOT~~ AIR MODEL AT ITS THREE SECTIONS A, B AND C

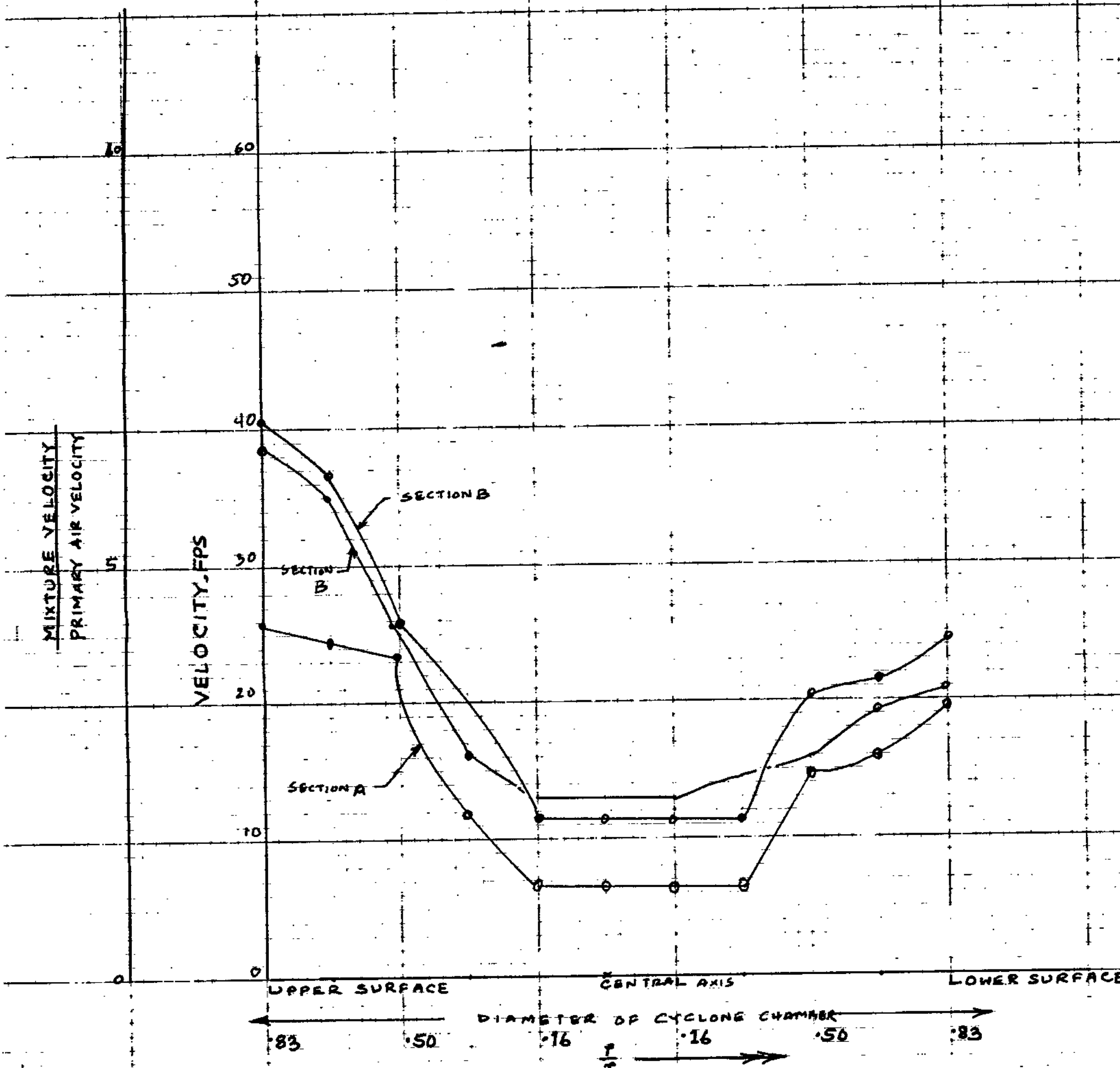

Fig. 6.[illegible] AXIAL VELOCITY DISTRIBUTION OF [illegible] AIR INSIDE THE CYCLONE CHAMBER OF [illegible] AIR MODEL AT ITS SECTIONS A, B AND C

EFFECT OF FUEL SIZE ON THE FLOW OF PRIMARY AIR

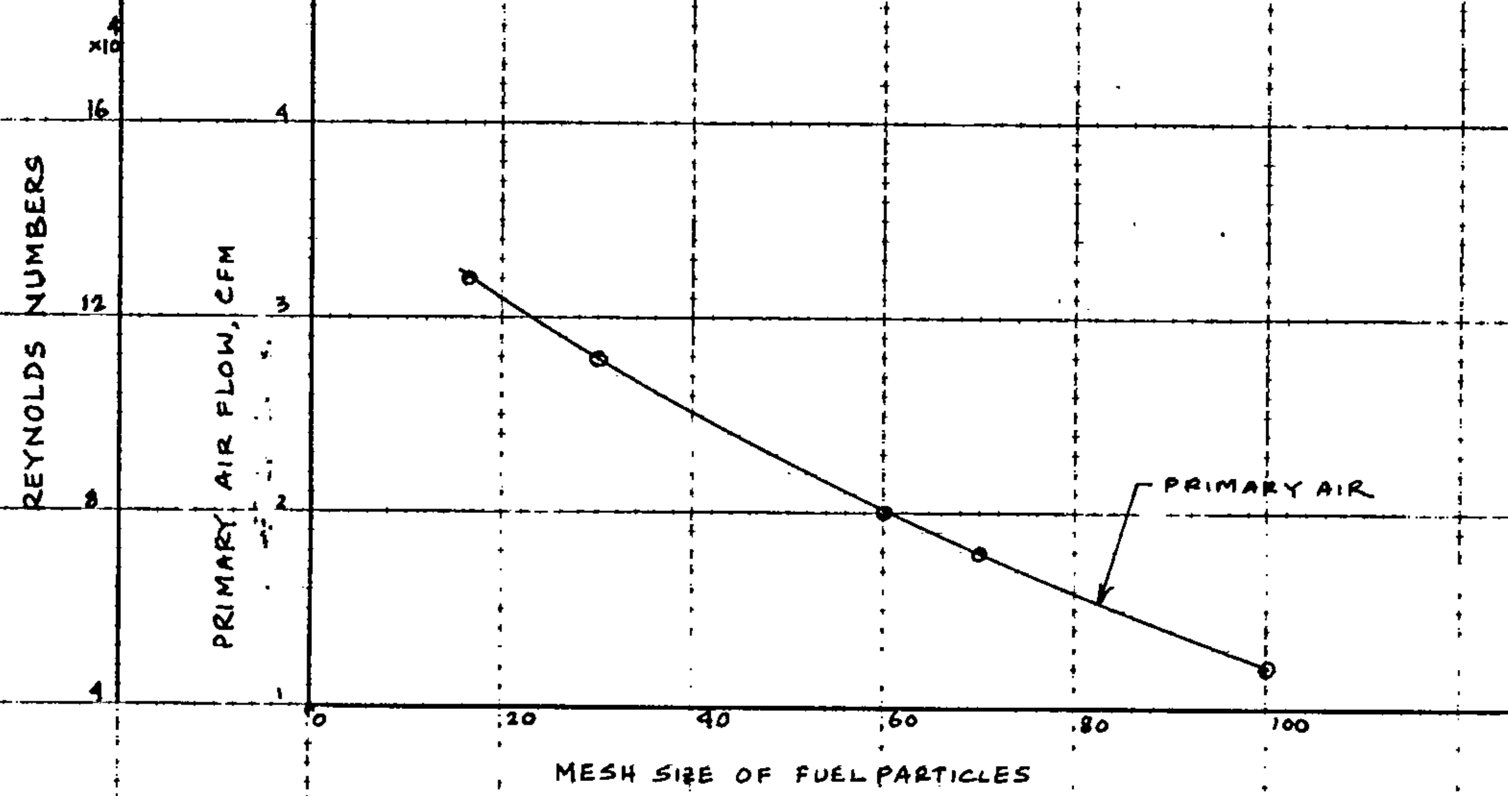

Fig. 6-3

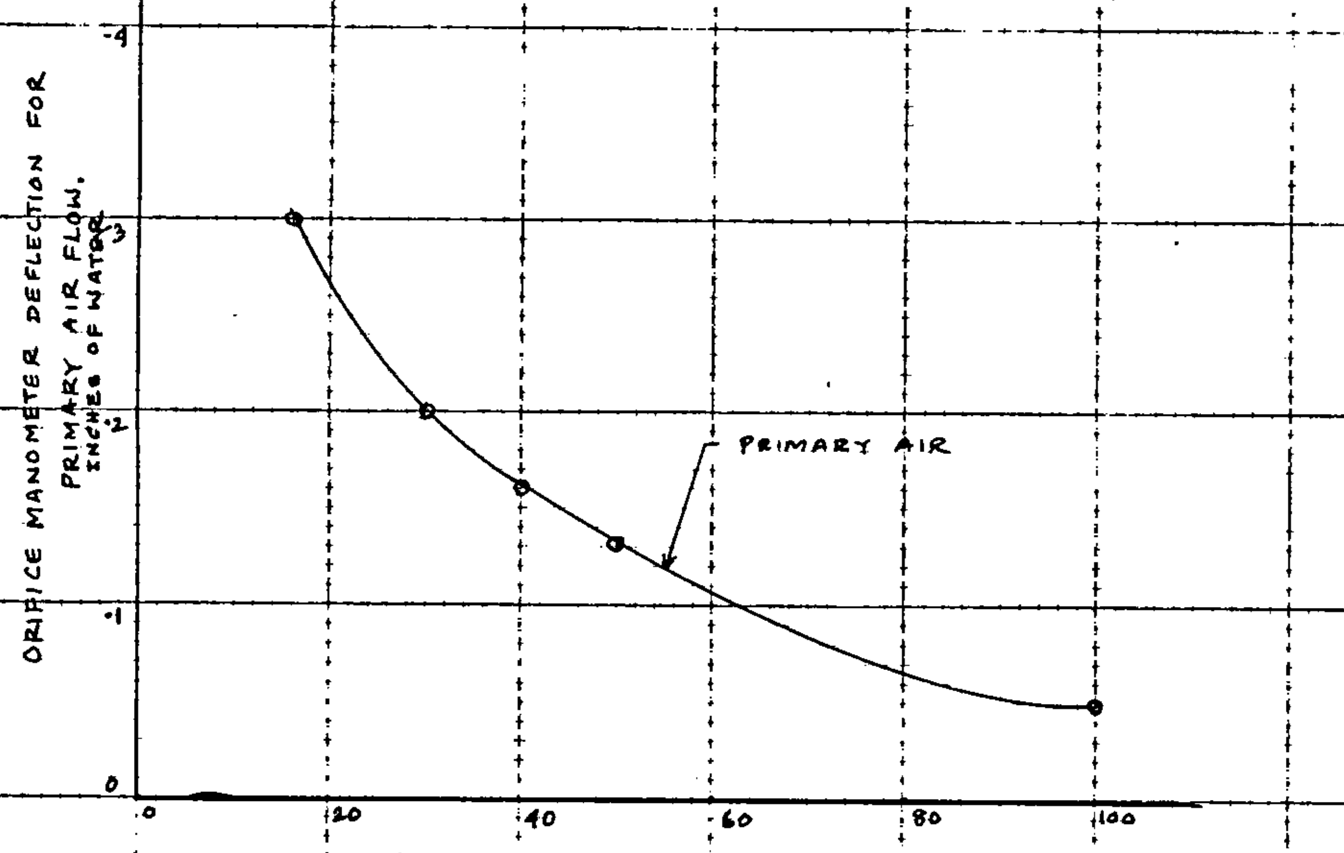

FIG. 6-4

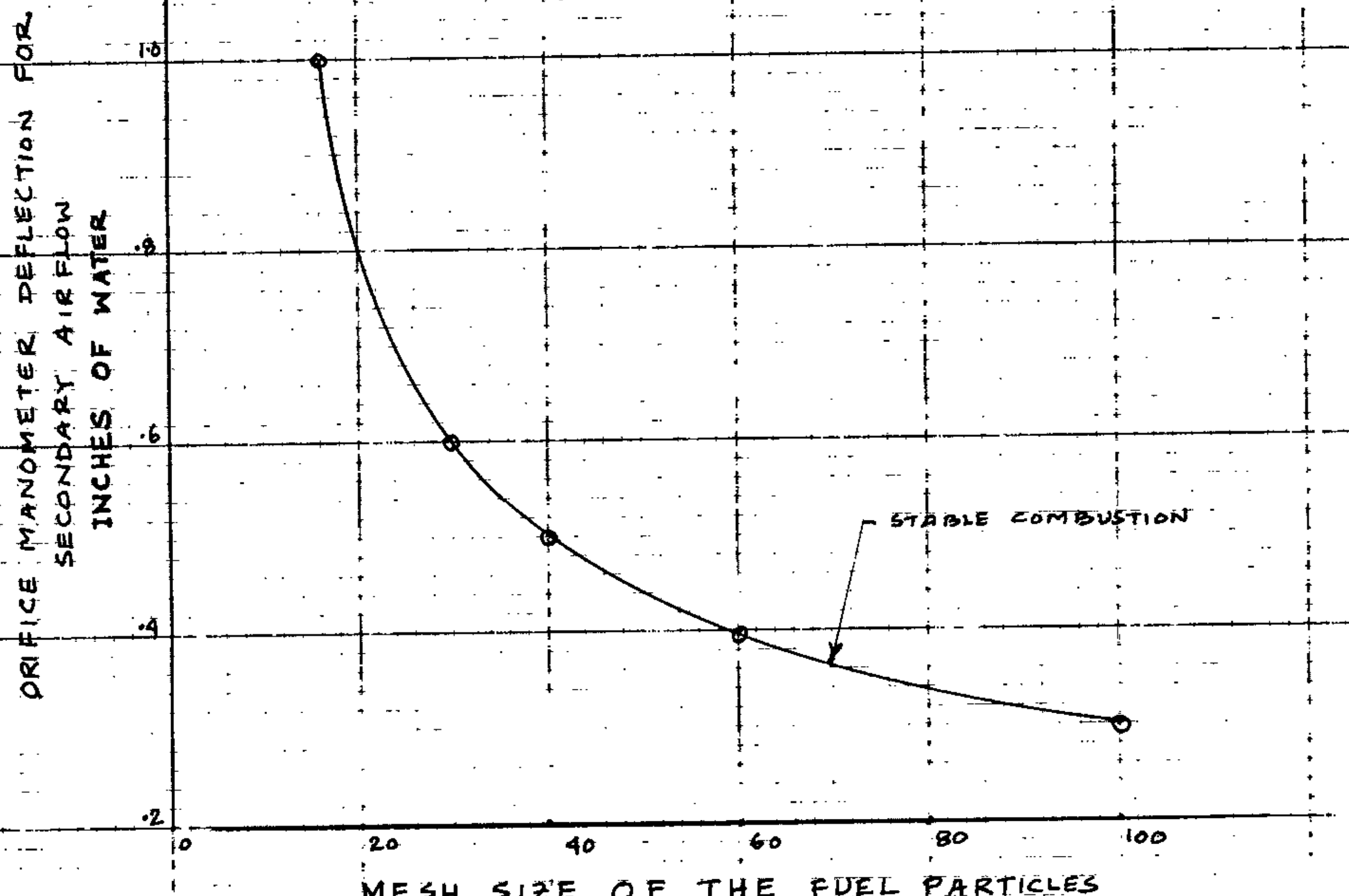

Fig. 6-5 SECONDARY AIR FLOW FOR STABLE COMBUSTION

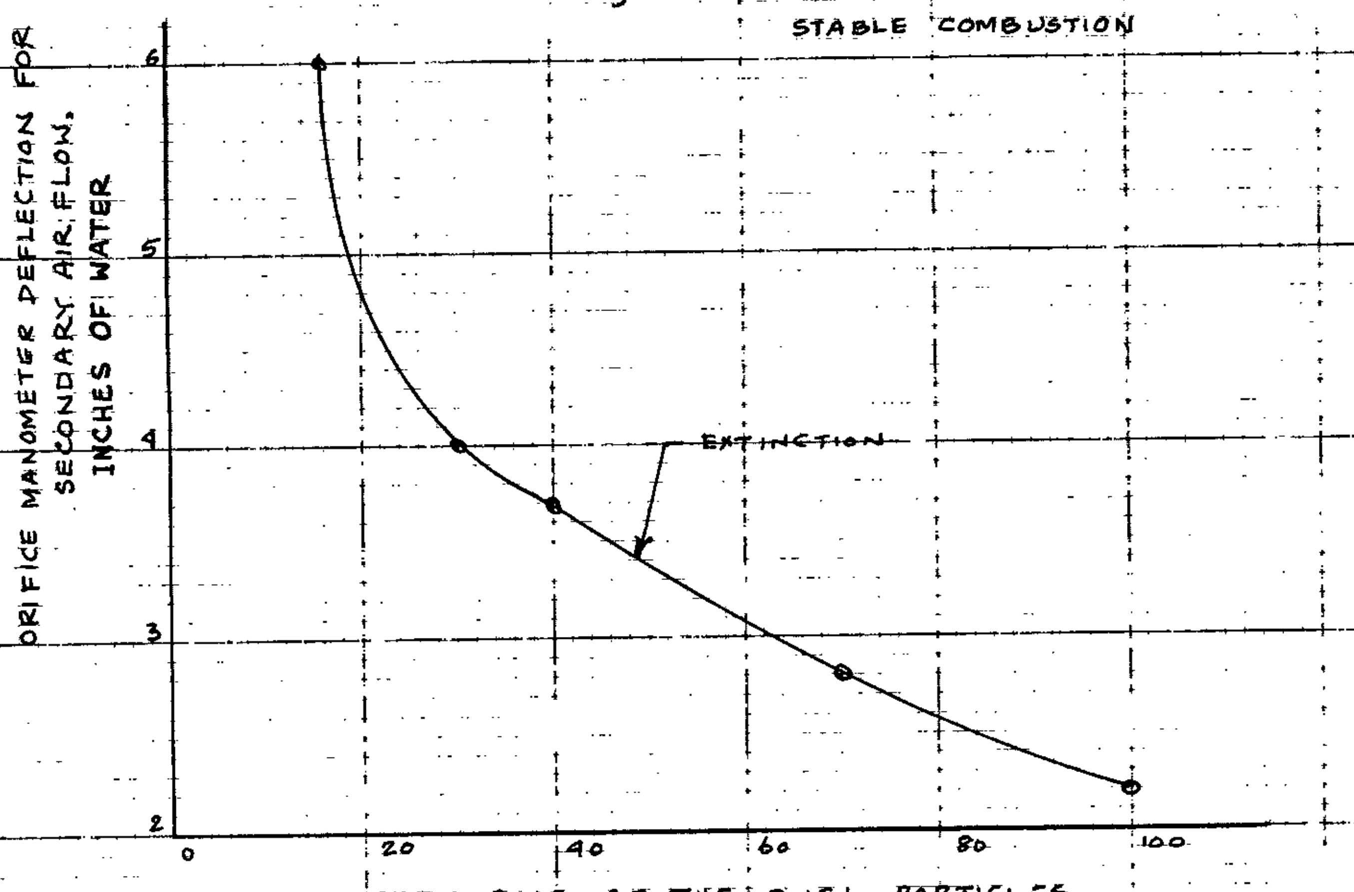

Fig. 6-6 SECONDARY AIR FLOW FOR EXTINCTION

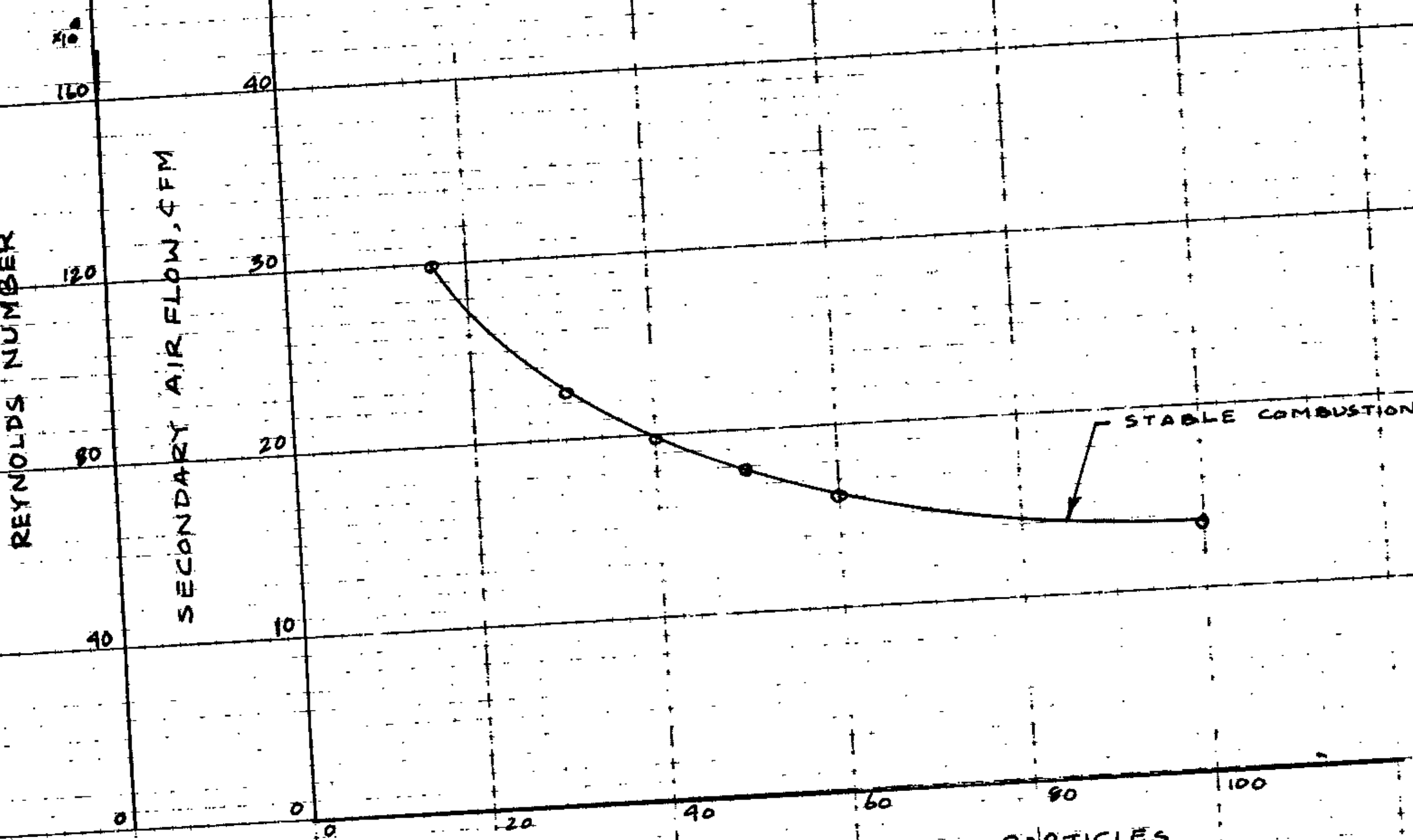

FIG. 6-7 SECONDARY AIR FLOW FOR STABLE COMBUSTION

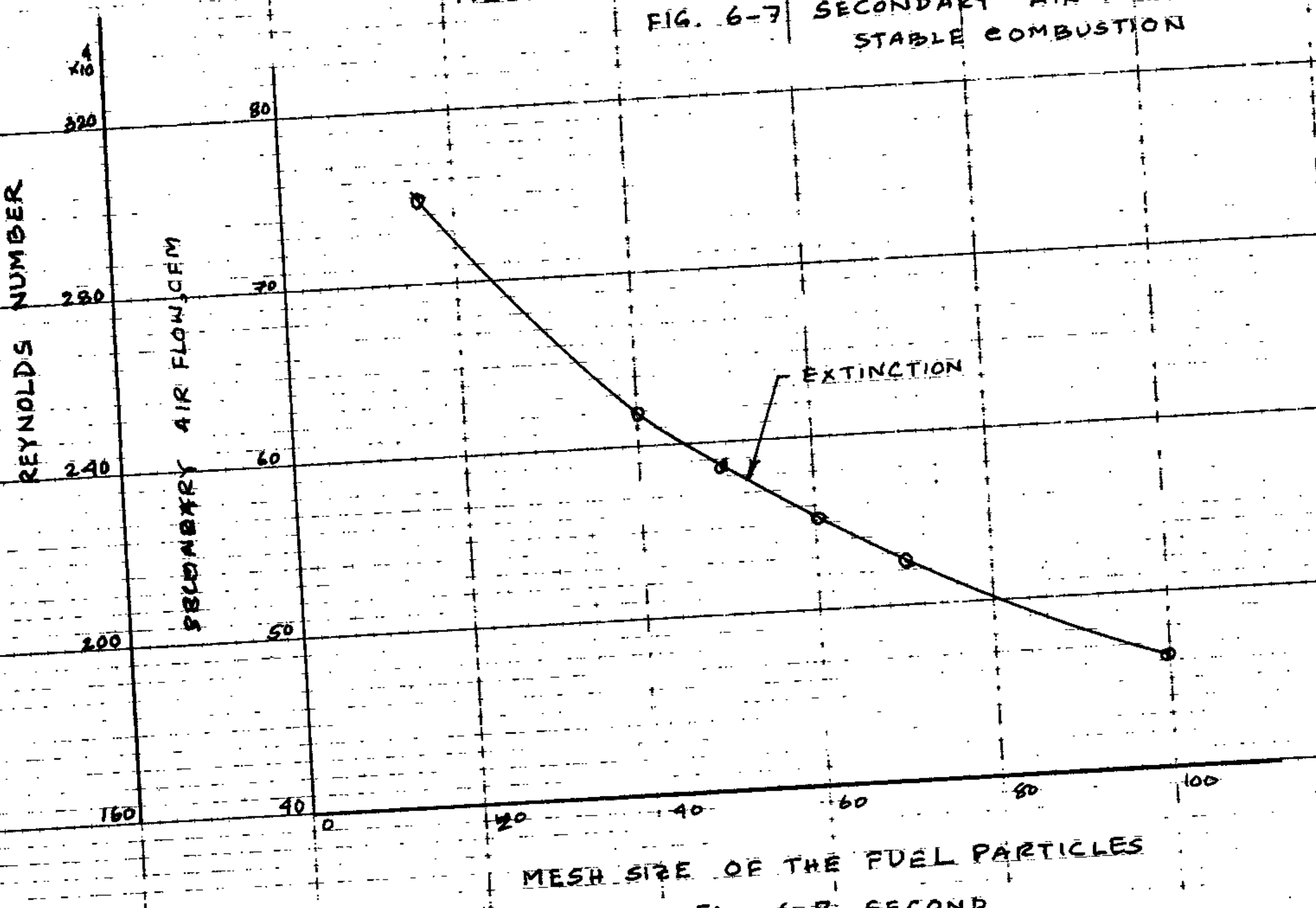

Fig. 6-8 SECOND

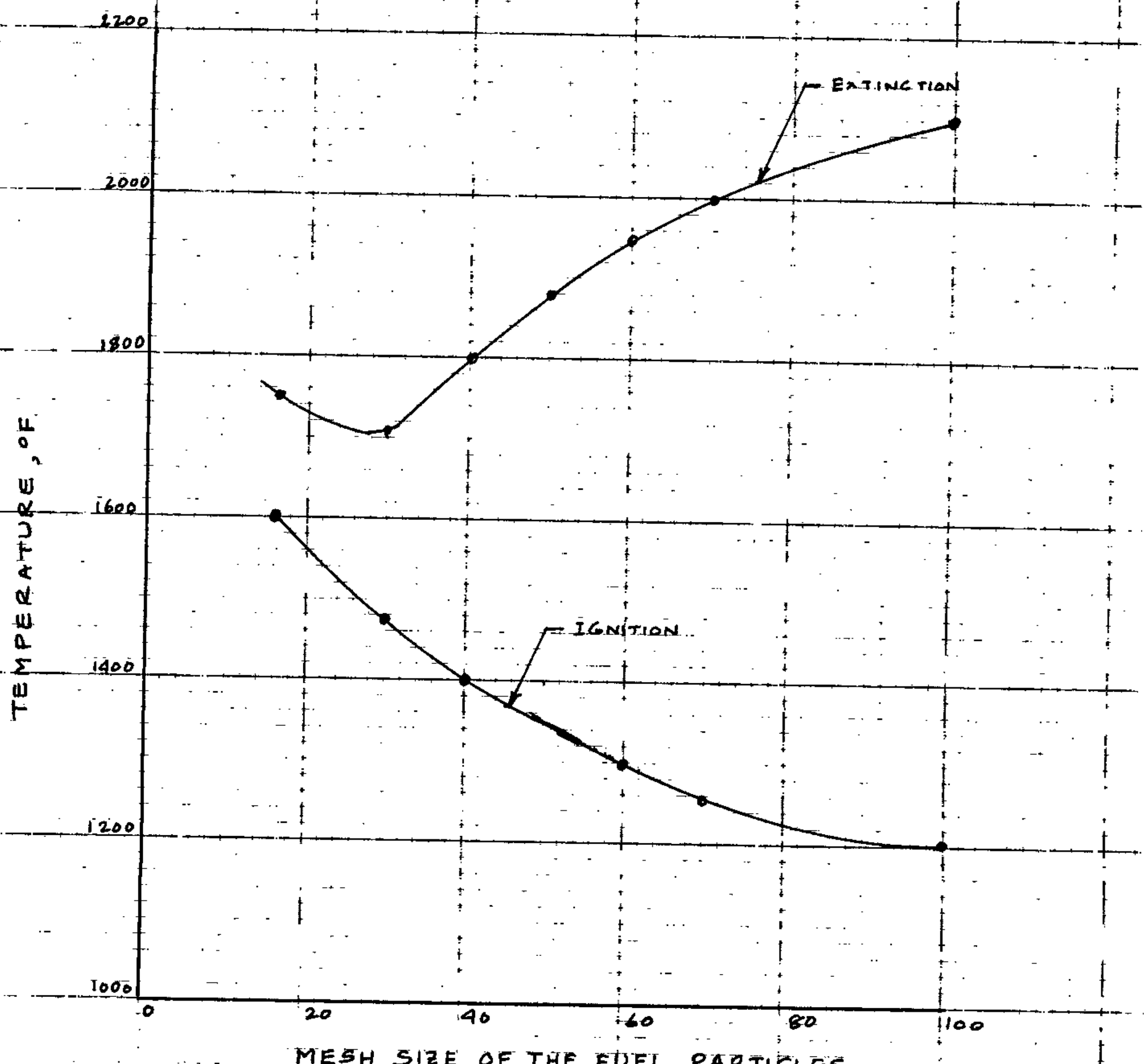

Fig 6.9 EFFECT OF FUEL SIZE ON THE TEMPERATURE OF IGNITION AND EXTINCTION

Fig. 6-10 RADIAL TEMPERATURE DISTRIBUTION (HOT AIR MODEL)

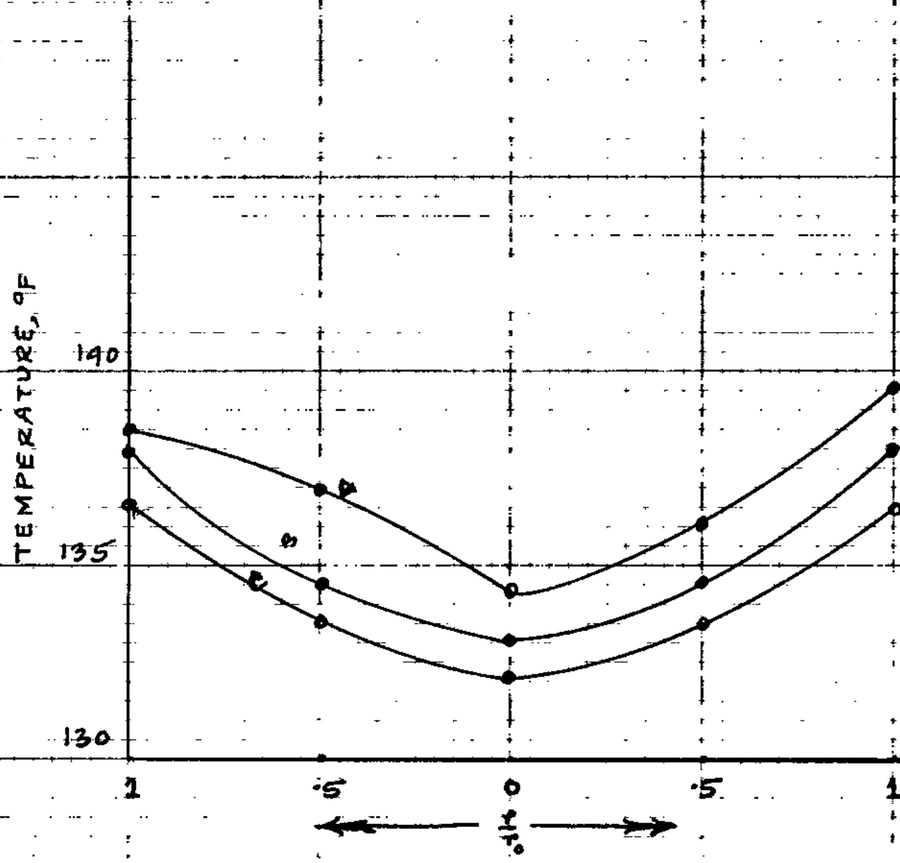

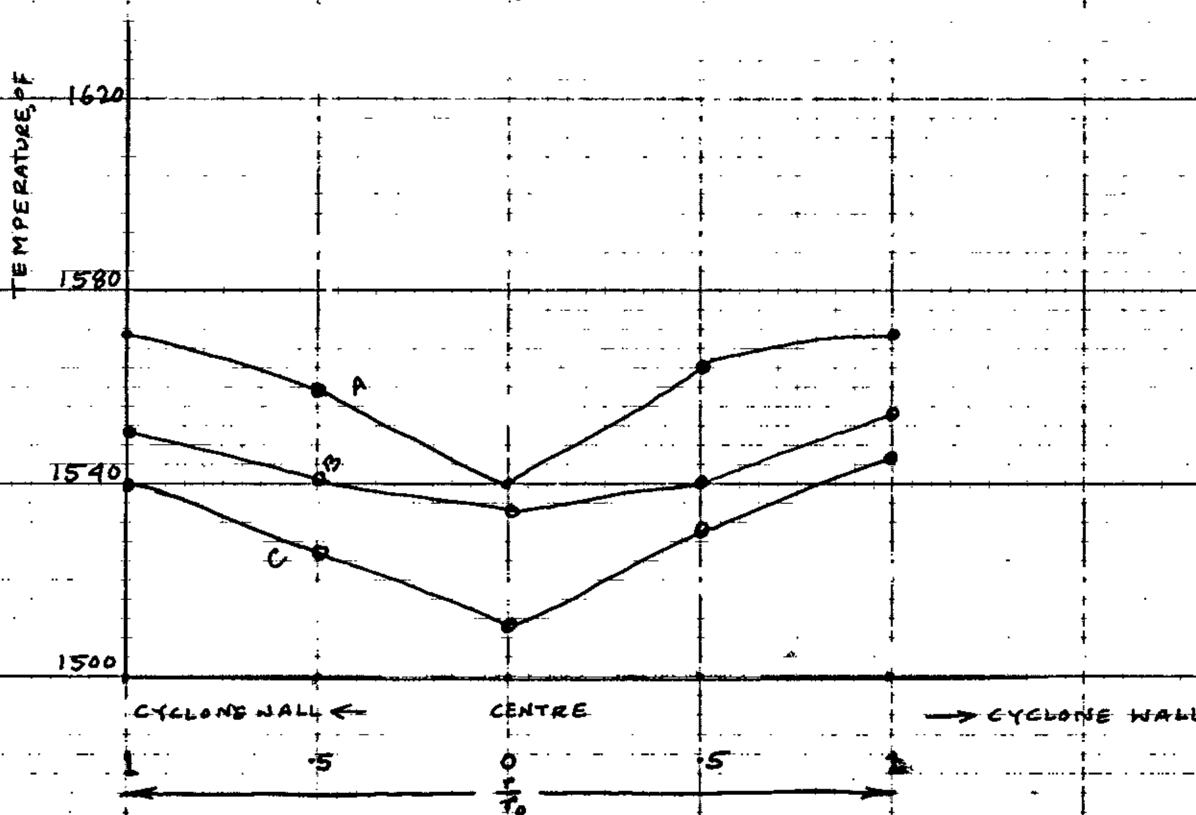

Fig 6-11 RADIAL TEMPERATURE DISTRIBUTION PROTOTYPE FURNACE

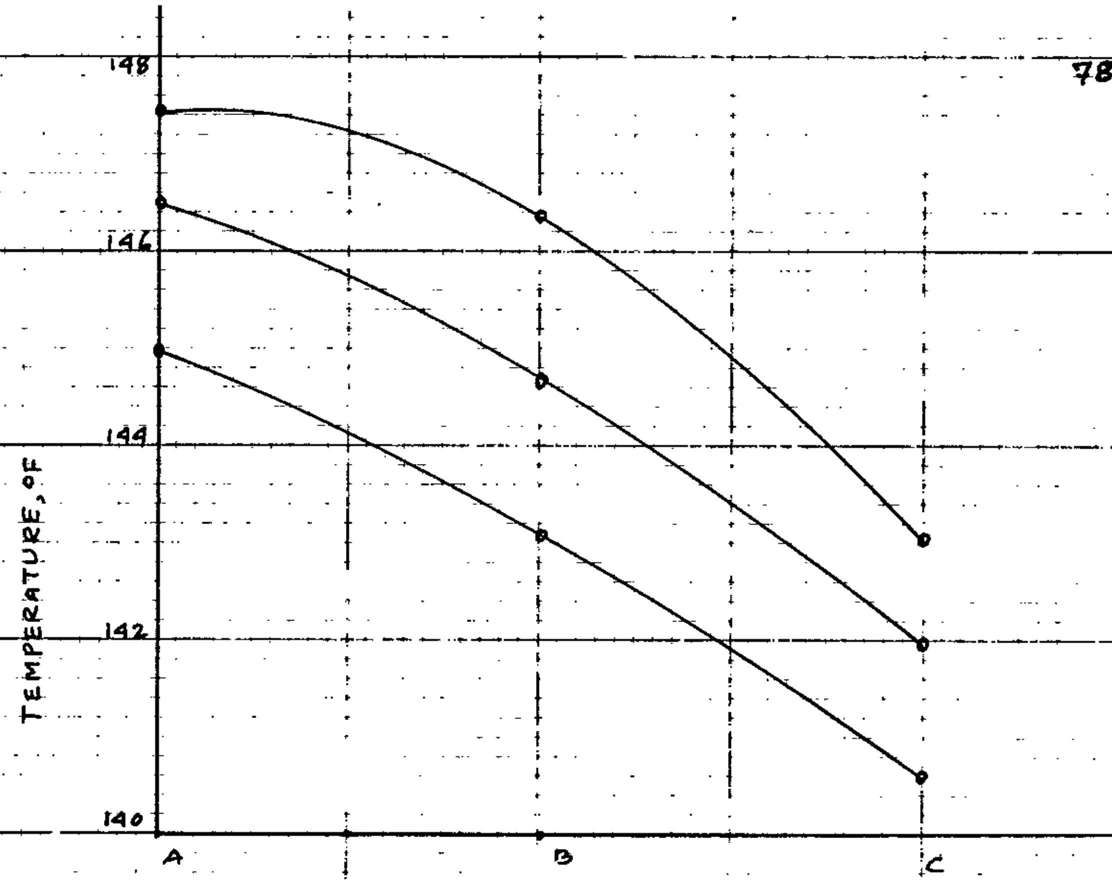

Fig. 6-12 TEMPERATURE DISTRIBUTION ALONG THE LENGTH OF CYCLONE CHAMBER, (HOT AIR MODEL)

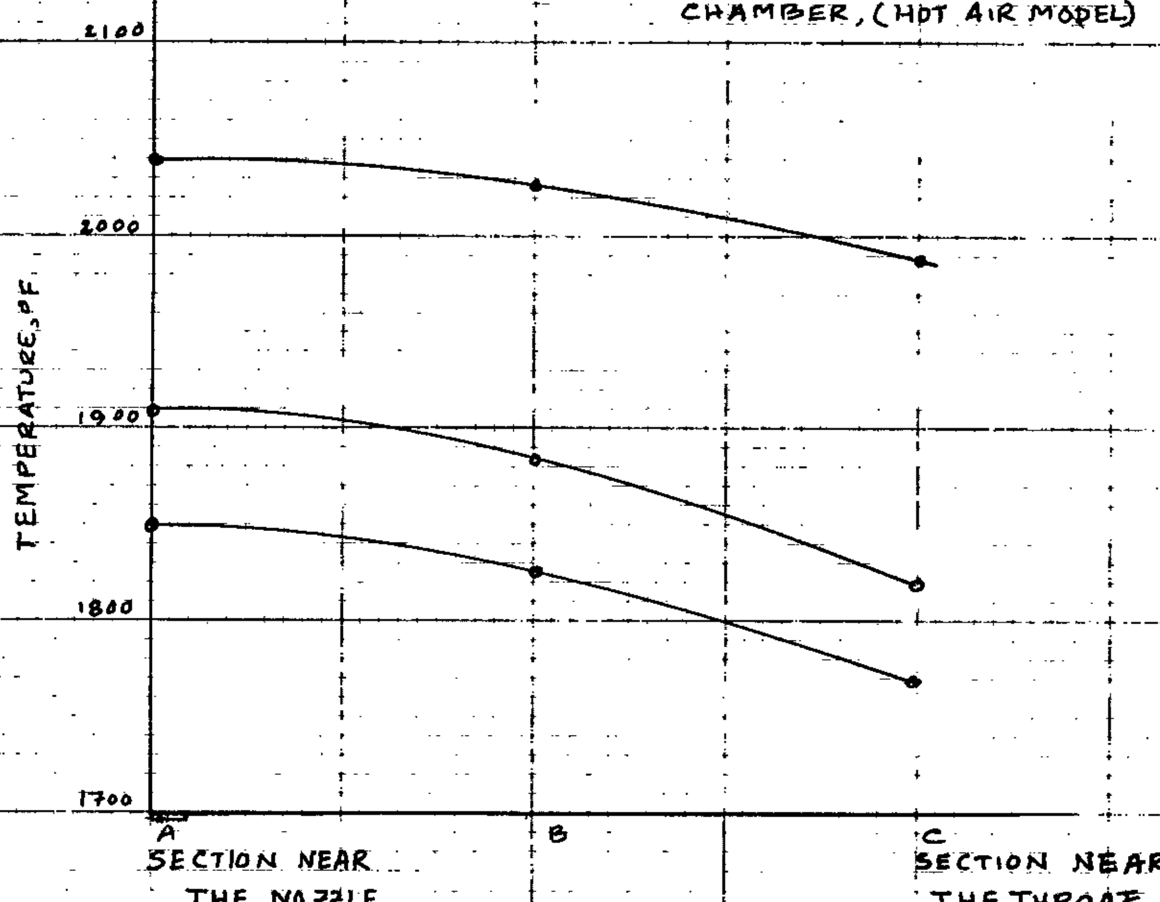

Fig. 6-13 TEMPERATURE DISTRIBUTION ALONG THE LENGTH OF PROTOTYPE FURNACE

CHAPTER VII

DISCUSSION AND CONCLUSION

7.1 The experimental investigation concerns the performance of an experimental horizontal cyclone combustion chamber, built up by the author. The cyclone chamber was used as a cold air model and a hot air model, as well as as a prototype combustion furnace, and the present discussion relates mainly to their behaviour. In contrasting the behaviour of the cold air and hot air models, the axial flow pattern of the air and some of the pressure losses in the cyclone chamber have been presented. As a prototype furnace, the conditions for satisfactory transport of fuel particles in suspension in primary air have been analysed. The theory of modeling as applied to air models and prototype furnace has been discussed in connection with the flow pattern, intensity of turbulence, and the temperature distribution in the models and combustion furnace. In this context, the relevant similarity criteria relating to intensity of turbulence, radiation heat transfer, flame contour and temperature distribution have been intrоduced. Finally, the combustion characteristics of the prototype cyclone furnace have been set forth. This part of the analysis is devoted largely to the study of the effect of secondary air velocity and size of the fuel particles on the process of combustion with special reference to phenomenon of ignition and extinction, and to the study of the effect of fineness of the fuel particles on the size of the flame, rate of combustion and the time of burning. The processes of kinetic and diffusion combustion occurring in the prototype furnace have also been differentiated.

7.2 Using the small experimental horizontal cyclone furnace as a cold air model, it has been endeavoured to study the flow pattern of the mixture of primary and secondary air inside the cyclone chamber. Since the furnace chamber was cylindrical and the admission of air was tangential, the direction of flow was somewhat defined. From pitot tube traverses, it has been observed, in general, that the velocity of air had more than one component. From a horizontal and a vertical traverse of the velocity probes, the tangential and the axial velocities were found to be more significant. The tangential velocity was studied only at the nozzle point.Due to experimental difficulties of traversing the pitot tubes in tangential directions at other sections, only the axial flow pattern was studied at different sections of the furnace. Figure 6-1 shows the behaviour of axial velocity of cold air within the cyclone chamber. A study of the axial velocity profiles at sections A, B and C of the cyclone furnace reveals that the flow of air was not circular. The velocities at the upper chamber surface and also at the lower surface were not similar at any section which clearly indicates that the flow was spiral. The velocity readings were appreciably larger near the cyclone wall and comparatively much smaller near the centre at which the velocities were more or less constant and also negligible. It was also found that flow of air occured in certain layers, indicative of cyclonic spiral flow.

7.3 The axial flow of air in the horizontal cyclone was studied for constant quantity of primary air but varying the quantity of secondary air. The flow of primary air was kept constant in the cold air models due to the fact that the primary air velocity was not varied in the prototype furnace from the optimum value for each fineness of the fuel particle size. The velocity profiles vary widely for different quantities of secondary air. It is therefore quite probable that the number of spiral was largely dependent on the velocity of secondary air. Cautius(8) also investigated the axial flow pattern in a horizontal cyclone furnace by burning diesel oil, coal and air and also by air only. The axial flow pattern of cold air obtained in the present investigation was more or less similar to that obtained by Cautius. Tissandier (40) studied the axial velocity profile in a cold aerodynamic model of the Ijmuiden pulverised fuel furnace. Tissandier's experimental plot of axial velocity was similar to the Figure 6-1. Tissandier derived a similarity criteria for axial velocities. He said that if λ is the ratio of the length of the isothermal model to the length of the real furnace, s_1 and s_2 are primary and secondary jet areas, then

$$\lambda = L_{model} / L_{furance}$$

$$s_{1\,model} / s_{1\,furance} = \lambda^2 \left(\frac{\rho_1}{\rho} \right)_{furnace}$$

$$s_{2\,model} / s_{2\,furance} = \lambda^2 \left(\frac{\rho_1}{\rho} \right)_{furnace}$$

Since we used the same cold air model as the furnace for combustion, it is therefore reasonable to expect that the velocity patterns will be similar in both cold air models and during combustion.

7.4 Accurate measurement of pressure losses in the cold air model involved much difficulties. In view of these, pressure loss at the nozzle was only studied. Static pressure at different sections of the furnace was also studied. From table, it was quite clear that the maximum pressure loss occurred at the nozzle point. In chapter 2, we discussed that the total pressure loss in the cyclone chamber is the summation of the pressure loss at the nozzle, pressure loss at the vortex and pressure loss during combustion. The pressure loss at the vortex and the pressure loss during combustion were not measured. In comparison with the nozzle pressure loss, it appears that the other pressure losses were very negligible. Theoretical equations for the pressure losses, set out in chapter 2 also give evidences for this prediction.

7.5 Using the small horizontal cyclone chamber as a hot air model, defined as the model where the secondary air was heated to a temperature of about 500 $^{\circ}F$ before it entered the cyclone chamber, the axial flow was studied with the constant primary air flow but varying the secondary air flow. The velocity profiles followed the similar trend as in the cold air model, but the velocities differed in magnitudes. With the hot air, velocities were appreciably higher because of the high temperature and hence, the smaller density of hot air. This is, ofcourse, to be expected from the equations of ideal gases. The pressure losses at the nozzle was also studied for the hot air flow. The results did not differ much from those of the cold air model.

7.6 Study of velocity pattern with the admission of fuel particles and air was not undertaken; since the finer fuel particles could easily block the pitot tubes. The fuel particles occupied less than 0.01% of the volume of the air requirement for combustion. Aerodynamically, such a suspension of fuel particles in air behaves like a gas. It is, therefore, expected that the flow pattern of fuel air mixture will behave similarly to that of the air alone.

7.7 Studies were undertaken to determine satisfactory condition for the transport of fuel particles in suspension in primary air. Figure 6-3 describes the primary air velocity for carrying the fuel particles uniformly into the combustion chamber. Tables X to XIII illustrate that uniform fuel flow largely depend on the close adjustment of primary air velocity and percentage fuel valve opening. Certain optimum velocity of primary air and certain optimum opening of the fuel control valve made the flow uniform into the cyclone chamber.The limiting size of the fuel particles as obtained in the present investigation lies between 8-mesh and 100-mesh. The limiting size of the fuel particles,as calculated from the theoretical equations, set out in chapter 2, also lies within this range. It was worth noting that since certain optimum primary air velocity and certain optimum fuel valve opening made the fuel particles flow unoformly, the fuel rate was also optimum for the present set-up. To increase the fuel rate and also to burn any size of corser and finer fuel particles, gravity-controlled fuel-feeding system would have to be changed. Hence primary air velocity was not varied from the optimum value for each fineness of fuel particle size.

7.8 In an attempt to predict the performance of prototype cyclone combustion furnaces, theory of modeling was applied to small cyclone chamber used as cold and hot air model. As was discussed in chapter 4, similarity criteria that are to be satisfied for the fluid regime are the pressure co-efficient, the Reynolds number and the Froudes group. It was also established that if we use the same fluid in the model and prototype, the flow pattern in both the cases will be similar.Furthermore,if the operating temperature of the prototype furnace is maintained in the hot model, the model and the prototype combustion furnaces will have similar temperature profiles. Experimental results with the prototype cyclone furnace did not yield the expected similarity of flow patterns as in the cold air and hot air model. It is concluded that the flow patterns of the air models and the prototype furnace are not exactly similar because of the phenomenon of turbulence associated with the combustion of fuel. The intensity of turbulence was found to increase considerably during combustion. Owing to high heat release during combustion, temperature rose very sharply. Specific volume of the gases increased. Swirling motion was highly influenced by this tendency of the gases to expand.It was observed during combustion that turbulence was more developed in the later part of the combustion chamber. It was not so intense with the cold air model or hot air model. In both the models and prototypes, Reynolds number and the Froudes group were well-above the critical values.Although in the theory of modeling, it was said that for high velocity flows, Froudes and Reynolds number could be ignored safely.

From the results of the present investigation, this can not be accepted. Though the Reynolds number is the parameter controlling flow patterns, it is also not enough that Reynolds number of models and prototype,based on incoming air should be equal. Reynolds similarity is well-established for isothermal models only. In a furnace where combustion taking place, there is a continual change in Reynolds number which can not be simulated in a geometrically similar model. To have the similar flow pattern, the same intensity of turbulence should be maintained in the cold air model or hot air model as in the prototype furnace.

7.9 In chapter IV on modeling of cyclone combustion, we have seen that Lewis number for the combustible mixture is often taken slightly less than unity. It was also said that in many other systems it is very nearly unity. This can not be accepted in the present investigation since, in the rear part of the prototype furnace process of diffusion combustion was quite predominant during combustion of coarser fuels. It is, therefore, necessary to consider Lewis number in both air models and prototype furnace.

7.10 It can be seen from Figures 6-10 and 6-12 that the temperature distribution of hot air model are similar in some instances with those of the prototype furnace but in other instances different. Figures 6-12 and 6-11 illustrate the temperature distribution along the length of hot model. It is found that the temperature of air dropped as it circulated towards the throat. Figure 6-13 shows the temperature distribution inside the prototype furnace during combustion. The temperature drop along the length was due to heat loss and increasing amount of turbulence in the latter part of the cyclone combustion chamber. Though the temperature profiles followed the similar trend, the magnitudes were widely different. In chapter IV, it was discussed that if the hot model is run at the furnace operating temperature, the temperature profiles will behave similarly. In our experimental investigation the temperature of hot air was much below the temperature of the combustion gases. It is, therefore, quite likely that the temperature profiles would vary widely.

7.11 Figure 6-10 and 6-11 illustrate the temperature distribution of the hot air model and the prototype furnace along the radius. From the graphical plots, it was found that the temperature of of the cyclone chamber surface was much greater than the temperature at its centre. The radial temperature distributions of the hot air model and the prototype furnace were not similar. The difference between the temperature of the furnace at the wall and at the centre was largely magnified in the case of prototype furnace. It was because of the effect of radiative heat transfer. In chapter IV, we have seen that Damkohlers dimensionless group ($\frac{UL}{cv}$) is a function of Thring's radiation group($\frac{\rho C_p V}{\sigma \epsilon T^3}$) and also the ratio of the absolute temperatures. In the cyclone chamber of hot air model, the radiation effect was very negligible. Moreover, the hot air model was not operated at the prototype furnace temperature. So it is concluded that the prototype furnace and the air model will have similar temperature profile if Thring's radiation group and also the ratio of the absolute temperatures are considered.

7.12 Study of the temperature profile of the actual furnace reveals that the majority of the fuel particles were burnt in suspension or in layers very close to the cyclone chamber wall. This fact goes in agreement with the theory of cyclone firing as discussed in chapter II.

7.13 In the theory of modeling of cyclone combustion, it was also established that the nozzle and the combustion chambers should obey the scale equation $a = \frac{L^2 \rho_s'}{\rho_o}$ to have the similar flame contours in model and prototype furnaces. Since in the present experimental investigation, the model itself was used as a prototype furnace, the question of considering the above scale equation for similar flame contours did not arise. However, in other cases, the above similarity criteria should also be be maintained to have the similar flame contours.

7.14 Study of the influence of secondary air velocity and size of the fuel particles on the process of cyclone combustion was made by firing the furnace with finer and coarser fuels. Figure 6-9 represents the effect of fuel size on the ignition temperature. It was found that coarser fuel ignited at much higher temperature whereas the finer fuel ignited comparatively at lower temperature. This is to be expected as the rate of heat transfer from air to fuel particles is a function of particle size and surface area. The air flow also affected the temperature of ignition to be varied for different sizes. Ignition temperature is also a direct function of the velocity of fuel-air mixture. Newall and Sinatt(37) investigated that the furnace temperature necessary for steady ignition of coal particles was of the order of 1500 F which was considerably higher than the ignition temperature of coal in a fuel bed. The ignition temperature of the fuel particles obtained in the present investigation was of the same order. Gosh, Basu and Roy (13) also studied the influence of various physico-chemical factors like coal and oxygen concentrations in the coal dust suspension,particle size, furnace temperature, etc., on the velocity of coal dust suspension. The minimum furnace temperature necessary for igniting the finer coals was obtained by Gosh as 1550 F. Our results are also in agreement with this value.

7.15 From theoretical considerations Traustel and Nusselt(38) presented equations for estimating the rise of temperature of coal particles prior to ignition. If a coal dust suspension at a temperature t_0, at zero time, be exposed to radiation from all directions at a temperature T_r , the temperature t of the coal particles will rise initially according to the relation

$$t = t_0 + \frac{3 \sigma \alpha T_r^4}{c \rho r} \theta$$

Where c is the heat capacity, ρ is the density and r is the radius of the coal particles, θ is the time, σ is the radiation constant and α is a geometric view factor. Some time after ignition the rise of particle temperature is given by the approximate relation :

$$t = t_0 + \sigma \alpha T_r^4 \left\{ \frac{N_r^2}{(N+1)^2 K} + \frac{3 \theta}{(N+1) c \rho r} \right\}$$

7.16 From the above two theoretical equations, it is found that temperature of the particle is inversely proportional to the radius of the particle, other parameters remaining constant. This is not in line with the results of our experimental investigations. Our results revealed that the ignition temperature increased with the decrease in fineness of the fuel particle size. Traustel and Nusselt did not define this temperature of the particle as ignition temperature. Moreover, their experimental conditions were completely different from ours. The effect of secondary air velocity was not at all accounted in their equations. Therefore, only conclusion that can be drawn is that there is some relation between the size of the fuel particles and the ignition temperature. More experimental data will be necessary for setting mathematical equations in this connection.

7.17 The experimental work provided further evidence for the known fact that at higher secondary air velocity the rate of combustion must be higher to maintain a stable flame. The popular conception that the more air that is supplied the more rapid the rate of combustion of solid fuels is not perfectly true. With the increase in secondary air velocity, the mixture was enriched with air. From the experimental observations it was found that rate of combustion did not increase above a particular secondary air velocity at which the temperature rise was maximum. Increasing the secondary air flow beyond this value resulted in the fall of temperature until the flame of combustion died out. Nicholls and others have shown that the mechanism of the relation between air supplied and rate of combustion is quite complex and subject to very definite restraining limits.

7.18 It was stated in chapter III on thermal aspects of cyclone combustion that the temperature of extinction is higher than the ignition temperature of the combustible mixture. This was also illustrated in Figure 3-1 in the $\omega - \theta$ co-ordinates. Figure 6-9 depicts the ignition and extinction temperature of the fuel - air mixture in the prototype furnace. It is found that our results are in agreement with the theoretical prediction made in the text of chapter III. It is also expected that with the increase in air velocity, heat release rate would be higher to sustain high temperature in the cyclone chamber during combustion.

7.19 It was found that the finer fuel particles of 40 -mesh to 100-mesh size were burnt in the earlier part of the combustion chamber and the coarser fuel particles of 8-mesh to 30-mesh size in the latter part of it. For the fuel particles of 8-mesh size to 30-mesh size, combustion started at the region very near to the throat. The complete combustion of the coarser fuel particles did not take place because of little stay time of the air fuel mixture inside the combustion space. In other words, the coarser fuel particles did not get sufficient time for complete combustion before they were escaped through the throat. Dr. R.H. Essen High( ) set up the equations of burning time for single particle in the form of two terms: a chemical control term and a physical control term. Thus

$$t_b = K_c d_o + K_D d_o^2$$

where t_b is the burning time, K_c and K_D are burning constants and d_o is the diameter of the fuel particle. With fairly large particles, it seemed clear that the chemical term was quite unimportant. With finer pulverised fuel sizes, the chemical term $K_c d_o$ becomes relatigely important. Spalding(32) also showed that the burning time of the fuel particle varies directly as the square of the diameter of the fuel particle. It is, therefore, clear that the burning time for the coarser particles, is considerably more. With a particular secondary air flow for stable combustion, of coarser fuels, increasing in the burning time means increasing the stay time of the air fuel mixture. To increase the stay time, it is, therefore, concluded that the length of the cylindrical cyclone combustion chamber would have to be increased for the combustion of coarser fuels.

7.20 It was observed in general that an increase in fineness of the fuel size accelerated the combustion of the fuel particles resulting in a shorter combustion flame. Maximum temperature was attained nearer the nozzle with finer fuel. Consequently radiation was higher particularly with a high proportion of secondary air.

7.21 In summary, the author has described the result of his investigation into the performance of an experimental horizontal cyclone combustion chamber used as cold air and hot-air models and also as a prototype furnace. The study of axial flow of air inside the cyclone chamber reveals that the axial flow pattern was somewhat similar for the models and the prototype furnace. It was also found that the flow in the cyclone chamber was spiral, the fluid flew in some layers very close to the cyclone wall with negligible flow through the central portion of the cyclone. Moreover, the intensity of turbulence varied in air models and prototype furnace; in the latter more turbulence was developed because of high heat release and radiative heat transfer. The prototype cyclone furnace and the hot air models also did not yield the expected similarity of the temperature distribution inside the cyclone chamber. To predict the results of the prototype furnace from the hot air model study, it is therefore, concluded that high intensity of turbulence, radiative and convective heat transfer associated with high rates of heat release must be taken into account. It was found from the studies of transport of fuel particles in suspension in primary air into the combustion chamber of the prototype furnace that there was certain optimum primary air velocity for uniform transport of the fuel particles of particular fineness. Study of combustion characteristics of the prototype cyclone furnace has revealed that the size of the fuel particles and also the secondary air velocity highly influence the ignition and extinction phenomena of cyclone combustion. Ignition temperature increased with the decrease in fineness of the fuel particles. The extinction temperature was in general, higher than the ignition temperature.Increase in fineness in fuel size produced shorter flame and increased the rate of combustion. The burning time was more for coarser fuel. Finer fuel particles were burnt in the earlier part of the combustion chamber and coarser fuel particles in the rear part of it. It is,therefore, anticipated that kinetic combustion occurred near the nozzle and diffusion combustion occured near the throat of the cyclone combustion chamber. The experimental furnace is an excellent tool for further investigations.

A P P E N D I X 'A'

Experimental Data.

Tabulated Results.

TABLE I

5			7			9			11		
A	B	C	A	B	C	A	B	C	A	B	C
.18	.20	.15	.15	.26	.23	.16	.39	.34	.20	.47	.44
.10	.16	.14	.13	.25	.20	.14	.31	.29	.16	.37	.37
.06	.12	.06	.12	.17	.10	.13	.16	.15	.10	.26	.20
.03	.05	.04	.08	.06	.05	.03	.01	.06	.09	.11	.06
.02	.01	.04	.06	.04	.02	.01	.03	.04	.08	.02	.06
.02	0.0	.04	.06	0.0	.02	.01	.03	.04	.08	.02	.01
.02	0.0	.05	.06	0.0	.02	.01	.03	.04	.08	.02	.01
.02	.005	.06	.06	.02	.05	.02	.02	.05	.08	.02	.01
.02	.01	.07	.07	.04	.06	.05	.10	.06	.09	.08	.05
.04	.08	.10	.08	.05	.07	.06	.11	.09	.10	.12	.08
.10	.17	.15	.08	.15	.10	.09	.14	.10	.12	.15	.11

TABLE II

	5			7			9			91	
A	B	C	A	B	C A	A	B	C	A	B	C.
.16	.23	.17	.18	.28	.26	.19	.41	.35	.23	.50	.45
.14	.17	.15	.14	.26	.21	.16	.38	.30	.18	.40	.38
.08	.13	.09	.13	.18	.11	.14	.20	.18	.15	.29	.25
.04	.07	.05	.09	.07	.06	.04	.08	.07	.10	.15	.08
.03	.02	.05	.07	.05	.03	.01	.04	.04	.04	.09	.08
.03	0	.05	.07	0	.03	.01	.04	.04	.09	.04	.02
.03	0	.05	.07	0	.03	.01	.04	.04	.09	.04	.02
.03	.01	.06	.07	.02	.03	.01	.05	.04	.09	.04	.02
.04	.02	.08	.08	.08	.05	.06	.06	.06	.06	.10	.02
.04	.09	.11	.08	.05	.08	.06	.10	.09	.12	.09	.08
.11	.18	.16	.09	.17	.12	.10	.15	.11	.14	.16	.13

TABLE III

		A				B				C			
		1	2	3	4	1	2	3	4	1	2	3	4
1	1.3	.02	.01	.02	.01	.01	.01	.01	.01	.0.1	.01	.01 .01	.025
2	2.8	.02	.03	.04	.01	.03	.03	.04	.02	.03	.04	.04	.05
3	4.3	.05	.06	.05	.04	.05	.05	.05	.05	.05	.05	.05	.05
4	5.6	.06	.09	.13	.04	.07	.08	.08	.07	.06	.07	.06	.06
5	6.4	.10	.12	.14	.05	.09	.09	.09	.09	.13	.11	.10	.115
6	7.5	.11	.15	.20	.09	.14	.135	.135	.13	.24	.14	.13	.18
7	8083	.14	.29	.20	.05	.15	.17	.17	.155	.245	.16	.145	.18
8	12.3	.18	.26	.24	.17	.17	.17	.18	.19	.245	.20	.17	.13
9	13.1	.19	.29	.40	.20	.30	.32	.33	.31	.28	.29	.29	.32
10	15.4	.31	.45	.50	.22	.32	.34	.34	.36	.29	.30	.32	.37

TABLE IV

	A				B				C				
	1	2	3	4	1	2	3	4	1	2	3	4	
1	1.5	.02	.02	.03	.02	.02	.02	.02	.02	.02	.02	.02	.025
2	2.7	.03	.04	.05	.05	.04	.03	.04	.04	.03	.035	.035	.035
3	4.1	.045	.06	.09	.04	.05	.06	.06	.045	.04	.035	.06	.06
4	5.6	.06	.09	.13	.04	.07	.075	.075	.07	.06	.065	.06	.08
5	7.1	.08	.12	.15	.06	.10	.10	.10	.09	.08	.09	.09	.11
6	888	.11	.16	.21	.08	.14	.14	.13	.13	.11	.12	.12	.135
7	9.8	.14	.19	.25	.10	.17	.16	.16	.14	.145	.15	.15	.15
8	11.3	.13	.21	.31	.11	.20	.19	.18	.18	.18	.18	.17	.20
9	12.7	.18	.26	.37	.13	.22	.22	.21	.20	.19	.22	.21	.25
10	14.1	.21	.29	.41	.14	.26	.24	.23	.23	.21	.25	.22	.25

TABLE V

Secy. Orifice Manometer readings	Opend End Manometer readings 16 in. before the nozzle	Pitot tube manometer readings at the tip of nozzle
0.5	0.7	0.8
1.0	0.4	1.6
1.5	1.9	2.3
2.0	2.9	3.4
2.5	3.5	4.2
3.0	4.3	4.9
3.5	5.1 5.9	5.9
4.0	5.9	6.7
4.5	6.6	7.8
5	7.1	8.1
7	10.4	11.7
9	13.1	14.8

Primary orifice manometer readings,	pPitot tube manometer readings at the tip of the primary nozzle
0.1	0.9
0.2	1.4
0.3	2.0
0.4	2.5
0.5	3.2
0.6	4.0
0.7	4.8
0.8	5.5
0.9	6.1

TABLE VI

Secondary orifice Manometer reading	Pitot tube manometer reading cold air	Pitot tube manometer reading Hot air	Millivolt correspon. to temp. of secy. air	Corrected Millivolt	Temp. F
0)5£	0.8	0.9	3.7	5.0	251
1.0	1.6	1.6	3.6	4.9	247
1.5	2.3	2.7	3.1	4.4	245
2.0	3.3	3.4	2.18	3.48	185
2.5	4.8	4.5	3.0	4.3	221
3.0	4.9	5.2	2.8	4.1	212
3.5	5.7	6.1	2.65	3.95	205
4.0	6.5	6.8	2.55	3.85	201
4.5	7.5	7.8	2.40	3.70	194
5.0	8.6	8.6	2.35	3.65	193
5.5	9.5	9.4	2.30	3.60	191
6.0	10.3	10.1	2.20	3.50	186
6.5	11.1	11.5	2.15	3.45	184
7.0	11.7	11.8	2.10	3.40	182
7.5	12.6	12.7	2.05	3.35	180
8.0	13.5	13.6	2.00	3.30	177
8.5	14.1	14.3	1.98	3.28	176
9.0 9.0	15.2	15.3	1.95	3.25	175
9.5	16.0	16.1	1.90	3.20	173

TABLE VII

	5	7	9	11	5	7	9	11	5	7	9	11
1	2.43	2.42	2.39	2.35	2.41	2.40	2.38	2.32	2.40	2.38	2.35	2.30
2	2.43	2.42	2.39	2.35	2.41	2.40	2.38	2.32	2.40	2.38	2.35	2.30
3	2.43	2.42	2.39	2.35	2,41	2.40	2.38	2.32	2.40	2.38	2.35	2.30
4	2.43	2.42	2.39	2.35	2.41	2.40	2.38	2.32	2.40	2.38	2.35	2.30

TABLE VIII

	A				B				C			
	5	7	9	11	5	7	9	11	5	7	9	11
1	6.7	6.31	5.83	5.54	6.6	6.22	5.85	5.51	6.41	5.1	5.72	5.46
2	6.71	6.31	5.83	5.54	6.6	6.21	5.83	5.50	6.42	6.1	5.71	5.46
3	6.7	6.31	5.83	5.54	6.6	6.20	5.80	5.50	6.45	6.1	5.71	5.46
4	6.72	6.31	5.83	5.54	6.62	6.30	5.82	5.52	6,42	6.1	5.72	5.46

TABLE IX

	0.5			1.0			1.5			2.0		
	A	B	C	A	B	C	A	B	C	A	B	C
1	2.4	2.4	2.35	2.6	2.43	2.50	2.65	2.60	2.55	2.68	2.62	2.60
2	2.36	2.30	2.30	2.55	2.40	2.48	2.60	2.58	2.53	2.65	2.60	2.55
3	2.30	2.31	2.20	2.52	2.50	2.45	2.55	2,55	2.50	2.60	2.58	2.50
4	2.35	2.30	2.30	2.55	2.40	2.48	2.60	2.58	2.53	2.65	2.60	2.55
5	2.42	2.40	2.35	2.60	2.43	2.50	2.65	2.60	2.55	2.68	2.62	2.60

	2.5			3.0			3.5			4.0		
1	2.60	2.55	2.50	2.58	2.54	2.50	2.55	2.50	2.45	2.50	2.50	2.44
2	2.58	2.50	2.48	2.55	2.50	2.45	2.53	2.48	2.42	2.49	2.47	2.42
3	2.52	2.50	2.45	2.50	2.45	2.40	2,50	2.45	2.40	2.48	2.45	2.41
4	2.58	2.53	2.58	2.55	2.50	2.45	2.53	2.48	2.42	2.49	2.47	2.42
5	2.60	2.55	2.50	2.58	3.54	2.50	2.55	2.50	2.45	2.50	2.50	2.45

TABLE X

Fuel Sige 8-16

Primy. Orifice Mano. Defl.	Fuel valve open- ning	Fuel carr- ied lbs.	Time of flow min.	Fuel Rate lbs/hr.
.15	25	1	30	2
.15	33.3	1.5	30	3.0
.15	41.6	1.7	30	5.4
.20	25	2.0	30	4.0
.20	33.3	2.5	30	5.0
.20	41.6	2.8	30	5.6
.25	25	2.9	30	5.8
.25	33.3	3	30	6
.25	41.6	2.5	30	5
.30	25	2.5	30	5
.30	33.3	1.5	30	3
.30	41.6	1.5	30	3

Fuel Size 16-30-Mesh.

Primy. orifice Man.Defl. Water.	Fuel Valve open- ing %	Fuel carried LB.	Time of Flow Min.	Fuel Rate lb/HR.
.10	33.3	3.5	30	7.0
.10	41.6	3.7	30	7.4
.10	50	4.0	30	8
.15	33.3	4.5	30	9.0
.15	41.6	4.6	30	9.2
.15	50	4.6	30	9.2
.20	33.3	4.8	30	9.6
.20	41.6	5	30	10
.20	50	4.9	30	9.8
.25	33.3	4.5	30	9
.25	41.6	4.5	30	9
.25	50	4	30	8

TABLE XI

Fuel Size : 30-40

Primy Orifice Mano. Deflt. Water	Fuel Value Openi-ng.	Fuel carr-ied LB.	Time of Flow Min.	Fuel Rate Lb/Hr.
.1	25	4	30	8
.1	33.3	4.5	30	9
.1	41.6	4.5	30	9
.15	25	5	30	10
.15	33.3	5.5	30	11
.15	41.6	5.7	30	11.4
.18	25	5.9	30	11.8
.18	33.3	6	30	12
.18	41.6	5.8	30	11.6
.20	25	5.5	30	11
.20	33.3	5.5	30	11
.20	41.6	5.3	30	10.6

Fuel Size 40-50

Primary orifice Mano.Deflt.	Fuel Valve Opening.	Fuel carried	Time of Flow	Fuel rate
.05	25	3	30	6
.05	29.2	3.5	30	7
.05	33.3	3.5	30	7
.10	25	4.5	30	9
.10	29.2	5.0	30	10
.10	33.3	5.5	30	11
.15	25	6	30	12
.15	29.2	6.5	30	13
.15	33.3	6.3	30	12.6
.20	25	5.8	30	11.6
.20	29.2	5.5	30	11
.20	33.3	5	30	10

TABLE XII

Fuel Size 50-60

Primary orifice Mano. Deflt. water	Fuel valve opening %	Fuel carried lbs.	Time of Flow Min.	Fuel rate lbs/hr.
.05	20.8	5	30	10
.05	25	5.5	30	11
.05	33.3	5.5	30	11
.10	20.8	6.5	30	13
.10	25	7	30	14
.10	33.3	6.8	30	13.6
.15	20.8	6	30	12
.15	25	6.2	30	12.4
.15	33.3	6.2	30	12.4
.20	20.8	5.8	30	11.6
.20	25	5.5	30	11
.20	33.3	5.5	30	11

Fuel size 60-70

Primary Mano. Deflt.	Fuel valve opening %	Fuel carried lbs.	Time of Flow min.	Fuel lbs/hr.
.05	18.5	5	30	10
.05	20.8	5.5	30	11
.05	25	6.0	30	12
.08	18.5	6.0	30	12
.08	20.8	7.5	30	15
.08	25	7	30	14
.10	18.5	6	30	12
.10	20.8	5	30	10
.10	25.0	5	30	10
.15	18.5	4.5	30	9
.15	20.8	4	30	8
.15	25.0	4	30	8

TABLE XIII

Fuel Size 70-100

Primary orifice Mano. Deflection	Fuel valve Opening	Fuel carried Lbs	Time of Blow, Min	Fuel rate lb/hr
.02	18.5	8.0	30	16
.02	20.8	8.3	30	16.6
.02	25	8.5	30	17.0
.05	18.5	10	30	17
.05	20.8	9.8	30	20
.05	25	9.5	30	19.6
.08	18.5	9.0	30	18
.08	20.8	9.0	30	18
.09	25	8.7	30	17.4
.10	18.5	8.0	30	16
0.10	20.8	7.5	30	15
0.10	25	7.5	30	15

TABLE XIV

Fuel size	Ignition temp. F	Extinction temp. F	Primary orifice manometer dflec.	Secy. orifice manometer deflection		Flow rate of fuel lb/hr
70-100	1200	2100	0.05	0.3	2.2	20
60-70	1250	2000	0.08	0.35	2.8	15
50-60	1300	1950	0.10	0.40	3.0	14
40-50	1350	1875	0.13	0.16	3.5	13
30-40	1400	1800	0.16	0.50	3.7	12
16-30	1475	1700	0.20	0.60	4.0	10
8-16	1600	1750	0.25	1.00	6.0	6

TABLE XV

24.2	29	25.1	25.1	33.2	31	25.9	40.5	38.6	29	44.5	42.3
20.3	25.9	24.2	23.3	32.4	29	24.2	37	35	25.9	39.4	39.4
15.9	22.4	15.9	22.4	26.7	20.3	23.3	25.9	25.1	20.3	33.2	29
11.25	14.5	12.9	18.6	15.8	14.5	11.3	20.3	15.9	19.5	21.5	15.9
9.15	6,45	12.9	15.9	12.9	9.2	6.45	11.3	12.9	18.6	9.2	15.9
9.15	0	12.9	15.9	0	9.15	6.45	11.25	12.9	18.6	9.15	6.45
9.15	0	14.5	15.9	0	9.3	6.5	11.3	12.9	18.6	9.2	6.54
9.15	4.54	15.9	15.9	9.15	14.5	6.45	9.15	14.5	18.6	9.15	6.45
9.15	6.45	17.6	17.6	12.9	15.6	14.6	20.3	15.9	19.5	18.6	14.5
12.9	18.6	20.3	18.6	14.5	17.6	15.9	21.5	19.5	20.3	22.4	25.1
20.3	26.7	25.1	18.6	25.1	20.3	19.5	24.2	20.3	22.4	25.1	21.5

Y

TABLE XVI

25.9	31	26.7	27.5	34.2	33.2	28.2	41.4	39	31	45.8	43.4
24.2	26.7	25.1	24.2	33.2	29.8	25.9	40	35.4	27.5	41	40
18.6	23.3	19.5	23.3	27.5	21.5	24.2	29	27.5	25.1	35	32.4
12.9	17.6	14.5	19.5	17.6	15.9	12.9	18.6	17.6	20.3	25.1	18.6
12.9	9.15	14.5	17.6	14.5	11.3	6.45	12.9	12.9	19.5	12.9	18.6
12.9	0	14.5	17.6	0	11.3	6.45	12.9	12.9	19.5	12.9	9.15
12.9	0	14.5	17.6	0	11.3	6.45	12.9	12.9	19.5	12.9	9.15
12.9	6.45	15.9	17.6	9.15	11.3	6.45	14.5	12.9	19.5	12.9	9.15
14	9.15	18.6	14.5	14.5	15.9	15.9	14.5	19.5	20.3	12.9	9.15
18.6	19.5	21.5	18.6	14.5	21.6	15.9	20.3	19.5	22.4	19.5	18.6
27.5	19.5	26.7	22.4	26.7	22.4	20.3	25.01	21.5	24.2	25.9	23.3

U

TABLE XVII

	A				B				C			
	5	7	9	11	5	7	9	11	5	7	9	11
1	140	139.5	138	136.5	139	138.5	137.6	135	138.5	137.6	136.5	134.4
2	140	139.5	138	136.5	139	138.5	137.6	135	138.5	137.6	136.5	134.4
3	140	139.5	138	136.5	139	138.5	137.6	135	138.5	137.6	136.5	134.4
4	140	139.5	138	136.5	139	138.5	137.6	135	138.5	137.6	136.5	134.4
1	327.5	310	288.5	275.4	323	306	289	274	314.5	300.5	283.5	271.6
2	328	310	288.5	275.4	323	305.5	288.5	273.5	315	300.5	283	271.6
3	327.5	310	288.5	275.4	323	305	287	273.5	316	300.5	283	271.6
4	328.5	310	288.5	275.4	323	309.5	288	274.5	315	300.5	283.5	271.6

TABLE XVIII

	0.5			1.0			1.5			2.0		
	A	B	C	A	B	C	A	B	C	A	B	C
1	[illegible]	138.5	136.5	147.4	140	143	149.5	147.4	145	150.6	148	147.4
2	137	134.4	134.4	145	138.5	142	147.4	146.5	143.4	149.5	147.4	145
3	134.4	134.7	130	144	133	140.5	145	145	145	147.4	146.5	143
4	136.5	134.4	134.4	145	138.5	142	138.5	142	147.4	146.5	143.4	143
5	139.5	138.5	136.5	147.4	140	143	149.5	147.4	145	150.6	148	147.4

	2.5			3.0			3.5			4.0		
	A	B	C	A	B	C	A	B	C	A	B	C
1	[illegible]	146.5	143	146.5	144.6	143	145	143	140.6	143	143	140.6
2	146.5	144.4	142	145	143	140.6	144.4	142	139.5	142.5	141.5	139.5
3	144	143	140.6	143	140.6	138.5	143	140.6	138.5	142	140.6	139
4	146.5	144.4	142	145	143	140.6	144.4	142	139.5	142.5	141.5	139.5
5	147.4	146.5	143	146.5	144.6	143	145	143	140.6	143	143	140.6

TABLE XIX

	70-100			60-70			50-60			40-50			30-40		
	A	B	C	A	B	C	A	B	C	A	B	C	A	B	C
1	1450	1625	1620	1655	1710	1650	1680	1780	1700	1690	1870	1740	1970	2060	1890
2	1430	1620	1615	1650	1620	1650	1660	1700	1650	1670	1855	1715	1910	1980	1875
3	1370	1600	1590	1630	1650	1620	1650	1710	1625	1650	1810	1700	1940	1950	1860
4	1440	1630	1600	1650	1700	1660	1670	1720	1650	1670	1850	1750	1950	1970	1880
5	1460	1650	1630	1650	1660	1700	1700	1790	1750	1680	1890	1780	1970	2050	1880

66666	0.5			1.0			1.5			2.0			2.5		
	A	B	C	A	B	C	A	B	C	A	B	C	A	B	C
1	1570	1550	1540	2020	2010	1950	2040	2020	1990	1910	1850	1820	1850	1825	1775
2	1560	1540	1525	2000	1990	1920	2020	2000	1950	1850	1800	1775	1830	1780	1740
3	1540	1535	1510	1970	1960	1910	1990	1970	1900	1805	1790	1750	1810	1775	1730
4	1565	1540	1530	1990	1980	1930	2020	2000	1940	1840	1800	1780	1835	1780	1745
5	1570	1555	1545	2030	2020	1970	2050	2030	2000	1900	1850	1810	1890	1830	1770

A P P E N D I X 'B'

* Specification of Fuel

@ Notation

* Bibliography

SPECIFICATION OF FUEL

Type	Peat (Coal)	
Proximate Analysis		
	Volatile Matter	56%
	Ash	12%
	Moisture	15%
	Fixed Carbon	17%
Calorific Value, Btu/lb		8250

NOTATION

Symbol	Quantity
a	cross sectional area of the jet
A	numerical constant in Arrhenius equation
b	$m_j/(m_{js}-1)$
B	transfer number
c	concentration of the combustible mixture
c	nondimensional concentration
c_p	specific heat at constant pressure
c_d	co-efficient of discharge
c_v	co-efficient of velocity
C	Sutherland constant
d	diameter of the fuel particle
D	diameter of the cyclone chamber
D	diameter of the nozzle tip
	diffusion co-efficient
E	activation energy
F_o	Characteristic factor
F_d	Drag force
F_c	centrifugal force
g	gravitational acceleration
G	jet momentum
H_w	heat flux per unit area
k	thermal conductivity
K	mass transfer co-efficient
l	active whirl length
L	length of the combustion chamber
m	mass of the fuel particle

Symbol	Quantity
m	fractional mass concentration
M	mass flow rate
N	actual mass of air-fuel/air
N_o	stoichiometric ratio of air-fuel/air
N_{Pr}, N_{Sc}, N_{Le}	Prandtlnumber, Schimdt number, and Lewis number respectively
p	pressure drop
q	heat of reaction
Q	quantityb of heat liberated
Q	flow rate
R	Universal gas constant
T	temperature of combustion
u,v,w	velocities in x,y, z directions
u	tangential velocity
U	reaction rate
v	exit velocity at the tip of the nozzle
v	radial velocity
V	volume
w	gas velocity field
w_f	coal rate
x,yz	rectangular space coordinates
α	angle
γ	specific weight
Δ	Laplacian operator
Δ	difference
η	r/x
θ	nondimensional temperature
μ	dynamic viscosity

Symbol	Quantity
ν	kinematic viscosity
ρ	density
ρ_f	density of the nozzle fluid in the prototype furnace
τ	time
τ_s, τ_K, τ_D	stay time, reaction time , diffusion time
$\tau_{sK}, \tau_{sD}, \tau_{DK}$	nondimensional times
φ	co-efficient of dompleteness of combustion

Subscripts

a	secondary air
b	at which the particle floats
c	combustion
cr	critical value
e	edge of the jet
f	coal
fg	flue gas
g	gas
I	ignition
E	Extinction
j	component of the mixture
m	middle og the cross section
N	nozzle
o	initial condition
O	at the cyclone wall
St.	stationary values
V	vortex

BIBLIGRAPHY

1. Ambrosius, E. E., and Robert, D. F., " Mechanical Engineering Laboratory Practice," The Ronald Press Company, New York, 1957.

2. Baker, D. H., Ryder, E. A., and Baker, N. H., " Temperature Measurement in Engineering," Vol. 1, John Wiley and Sons, Inc., New York, 1953.

3. Bowditch, F. W., " Some Effects of Turbulence on Combustion," Fourth Symposium on Combustion, pp. 674 -683 , 1953.

4. Bird, R. B., Stewart, W. E., and Lightfoot, E. N., "Transport Phenomena," John Wiley and Sons, Inc., New York, 1960.

5. Curtis, R. W., and Johnson, L.E., " Use of Flow Models for Boiler Furnace Design," Journal of Engg. for Power, 1959, Vol. 81, Series A, No. 4, pp.371-379.

6. Chesters,J.H.," The Aerodynamic Approach to Furnace Design," Journal of Engg. for Power, 1959, Vol. 81, Series A, No. 4, pp. 361-370.

7. Cautius, W., " Erfahrungen mit Horizontal - Zyklonfeuerungen," VDI-Verlag GMBH Dusseldorf.

8. Cautius, W., " Zwei Jahre Entwichlunsarbeit am Zyklon," Mitt. V.G.B. 1952, Nr. 21, 234.

9. Ducarme, J., Gerstein, M., and Lefebvre, A. H., " Progress in Combustion Science and Technology," Vol. 1, Pergamon Press, New York,

10. Flint, D., and Ray, W. D.," Procedure for Coal Sample Preparation," Journal of Institute of Fuel, 1958, Vol. 31, No. 206, pp. 123-132.

11. Gaydon, A. G., and Wolfhand, H. G., " Flames-Their Structure, Radiation and Temperature," Chapman and Hall Ltd., London, 1960.

12. Griffiths, E., " Methods of Measuring Temperature," Charles Griffith and Company Ltd., London, 1947.

13. Gosh, B.,Basu, D., and Roy, N.K., " Studies Of Pulverised Coal Flames," Sixth Symposium on Combustion, 1956, pp. 595-601

14. Hoy, H. R., Roberts, A. G., and Wilkins, D. M., " Some Investigations with a Small Cyclone Combustor," Journal of the Institute of Fuel, 1958, Vol. 31, No. 213, pp. 429-464.

15. How, M. E., " The Influence of Turbulence on the Burning Rates of Fuel Suspensions," Journal of the Institute of Fuel, 1966, Vol. 39, No. 303, pp. 150-159.

16. Hottel, H. C., and Person, R. A., " Heterogeneous Combustion of Gases in a Vortex System," Fourth Symposium on Combustion, 1953, pp.781-788.

17. Hattori, H., " Flame Propagation in Pulverised Coal-Air Mixtures," Sixth Symposium on Combustion, 1956, pp. 590-594.

18. Johnstone, R. E., and Thring, M. W.," Pilot Plants, Models and Scale-up Methods in Chemical Engineering," McGraw-Hill Book Company, Inc., New York, 1951.

19. Johnson, A. J., and Auth, G. H., " Fuels and Combustion Hand Book," McGraw-Hill Book Company, Inc., New York, 1957.

20. Knorre, G. F., and Nadzharov, M. A., " Zyklon-Feuerungen," 1958 Verlag Energietechn.,Moscow.

21. Lobscheid, Deutsche Babcock Wilcoxwerke; interne Ausarbeitung, 1951.

22. Lewis, B., and Elbe, G.V., " Combustion, Flames and Explosion of Gases," Academic Press Inc., New York, 1961.

23. Lorenzi, Otto de, " Combustion Engineering," Superheater, Inc., 1961.

24. Morse, F. T., " Power Plant Engineering," D. Van Norstand Co., Inc.,New York, 1949.

25. Madison, R. D., " Fan Engineering," Buffalo Forge Co., New York, 1959.

26. Martin, D.G. and Webb, J.D.," Simulation of Combustion Chamber Performance," Seventh Symposium on Combustion, 1959, pp. 651-653.

27. Ower, E., " The Measurement of Air Flow," Chapman and Hall Ltd., London, 1949.

28. Putnam, A. A., and Unger, E. W., " Basic Principles of Combustion Model Research," Journal of Engg. for Power, 1959,Vol. 81, Series A, No. 4, pp. 383-388.

29. Robertson, A.D.," Scaling and Modeling Criteria for Burner Design with Swirl Addition," Journal of the Institute of Fuel, 1966, Vol. 39. pp. 335-341.

30. Rosin, P. O., " The Mechanism of Combustion of Pulverised Fuel," Journal of the Institute of Fuel, 1958, Vol. 31, No. 211, pp. 346-355.

31. Seidl, H., " The Horizontal Cyclone as a Coal Burner," B. C. U. R. A. Gazette, London, 1962.

32. Smith, M. L., and Stinson, K. W.," Fuels and Combustion," McGraw-Hill Book Company, Inc.,New York, 1952.

33. Spalding, D. B.," Some Fundamentals of Combustion," New York Academic Press, Inc.,London, 1955.

34. Seidl, H., " The Development and Practice of Cyclone Firing," Institution of Mechanical Engineers, 1955, pp. 92-102.

35. Spalding, D. B.," The Art of Partial Modeling," Ninth Symposium on Combustion, 1963, pp. 833-843.

36. Thring, M. W., and Newby, M. P., " Combustion Length of Enclosed

Turbulent Jet Flames," Fourth Symposium on Combustion," 1952 pp. 789-795.

37. Sinatt, F. S. and Newall, W.,"Fuel," 3, 424,1924.

38. Traustel, S. and Nusselt, W. " Feuerungetech," 29,1941.

39. Siddal, R.G., " Use of Aerodynamic Models in the study of Industrial Furnaces," pp. 639-650, Seventh Symposium of Combustion 1958.

40. Tissandier, G., " Cold Aerodynamic Trials on a Fifth Scale Model of the IJmuiden Pulverised Fuel Furnace," Journal of the Institute of Fuel, Vol. 33, No. 235, 1960, pp. 377-399.

41. Vulis, L.A., " Thermal Regimes of Combustion," McGraw-Hill Book Company, Inc., New York, 1961.

42. Whitney, G.C.," Use of Flow Models for studying Pulverised Coal Burner Performance," Journal of Engg. for power, Vol. 81, Series A
4 No.4, pp.380-382.

43. Willians, F.A., " Combustion Theory," Addison-Wesley Publishing Company, Inc., London.

44. Weast, F.A.,Selby, S.M., and Hodgman, C.D., "Handbook of Physics and Chemistry," The chemical Rubber Company, Ohio, 1965.